A COMPUTATIONAL PARAMETRIC STUDY OF THE RELATIONSHIP BETWEEN THE CHARACTERISTIC GEOMETRY, FLOW STRUCTURE, AND HEMODYNAMICS OF INTRACRANIAL BIFURCATION ANEURYSMS

by

Michael J Durka

BS, University of Pittsburgh, 2011

Submitted to the Graduate Faculty of

the Swanson School of Engineering in partial fulfillment

of the requirements for the degree of

Master of Science

University of Pittsburgh

2013

UNIVERSITY OF PITTSBURGH

SWANSON SCHOOL OF ENGINEERING

This thesis was presented

by

Michael Durka

It was defended on

September 13, 2013

and approved by

Giovanni Galdi, PhD., Professor

Department of Mechanical Engineering and Materials Science

Paolo Zunino, PhD., Assistant Professor,

Department of Mechanical Engineering and Materials Science

Thesis Advisor: Anne Robertson, PhD., Professor,

Department of Mechanical Engineering and Materials Science

A COMPUTATIONAL PARAMETRIC STUDY OF THE RELATIONSHIP BETWEEN THE CHARACTERISTIC GEOMETRY, FLOW STRUCTURE, AND HEMODYNAMICS OF INTRACRANIAL BIFURCATION ANEURYSMS

Michael J Durka, M.S.

University of Pittsburgh, 2013

This work utilized computational numerical models in parametric studies to develop a relationship between the characteristic geometry of intracranial bifurcation aneurysms and the intra-aneurysmal blood flow structures. In general, intra-aneurysmal flow structures can be categorized by two flow types: Type I (one vortex) and Type II (two vortices). Flow structure can profoundly influence the intra-aneurysmal hemodynamic stresses, which are generally accepted as a major factor responsible for either the stabilization or the eventual rupture of intracranial aneurysms. However, there are currently no known reliable methods that can determine whether an aneurysm is prone to rupture. Current technology limits clinicians to the use of geometric data obtained via angiography as the only means of assessing rupture risk. Therefore, a method of obtaining a description of the intra-aneurysmal hemodynamics from aneurysmal geometry is a potentially valuable tool. Many studies conducted on this subject have the weaknesses of either assuming that one geometric parameter is sufficient to predict and describe intra-aneurysmal hemodynamics, or neglecting the combined effects of multiple parameters in studies involving more than one geometric parameter. Many of these studies are purely statistical and incorporate no mechanistic explanations or hypotheses for rupture. The work of this thesis considers the combine effects of multiple geometric parameters in a systematic manner which relates geometric parameters to flow structure, and flow structure to hemodynamic stress. By using this approach, an extensive systematic guide to intra-aneurysmal flow structure and hemodynamics has been developed which can readily offer clinicians a general description of intra-aneurysmal hemodynamic conditions in a clinical setting.

iv

Furthermore, the theory in this work can not only predict the existence of unfavorable hemodynamics, but can also identify the geometric feature(s) in particular that is (are) responsible for unfavorable hemodynamics. To provide evidence which can substantiate these notions, the predictive ability of the theory developed form the parametric study was tested by evaluating its ability to predict the flow structures in 27 clinical aneurysms. An evaluation of the theory's performance concludes this work.

TABLE OF CONTENTS

LIST OF TABLES

LIST OF FIGURES

PREFACE

I will first extend my appreciation to my thesis committee members Dr. Giovanni Galdi, Dr. Paolo Zunino, and Dr. Anne Robertson for their work and contributions toward this thesis. Furthermore, this work would not have been possible were it not for the gratefully appreciated contributions of the following.

Dr. Anne Robertson, my advisor, who, throughout my time as a graduate and undergraduate, has been an excellent mentor for me. Without her support and guidance, I would never have been in the position with the abilities to produce this thesis, nor would have I ever developed academically and professionally to the extent that I have done so under her mentorship. What she has done for me is invaluable, for which I am most grateful.

Zijing Zeng (now Dr. Zijing Zeng), a doctoral student of Dr. Robertson's during my time as an undergraduate, provided me with a wealth of knowledge and training with the entire CFD modeling process from the first stages of acquiring the model information to the meaningful organization of the post-processed results. He furthermore aided me with the finer details in the beginning stages of what would eventually become this work. This work would not have been possible for me to produce without the skills and techniques which I have learned from him.

Wenran Chen, an undergraduate student, diligently assisted me in producing many of the models for the validation study section of this work. Without his thorough, dependable work, I would certainly not have been able to finish this work in the comfortable time frame in which I had finished it.

Athif Wulandana, also an undergraduate, helped me with some final models and other work of mine while I was in the process of writing this thesis. Athif's assistance certainly made the process of writing this thesis more efficient by allowing me to fully concentrate on its production.

My gratitude is also extended to those who provided the clinical data used in the production of this work:

Finally, I will conclude my acknowledgments by thanking my family for all the support and nurturing they have given me throughout the years. For without them, all other acknowledgements made here would have been moot, as I would not be where I am today without my family.

1.0   INTRODUCTION

An intracranial aneurysm (IA) is a localized dilation or ballooning of a weakened blood vessel wall in the human brain. When the yield strength of the weakened aneurysm tissue becomes greater than the loading on the wall, the aneurysm ruptures causing subarachnoid hemorrhaging (SAH). The outcome of SAH from a ruptured intracranial aneurysm is often fatal or crippling, with 35%-50% mortality and 30% morbidity [1]. While the prevalence of IAs has been estimated to be roughly 2% for the general population, IA rupture is estimated to occur in only 0.01% - 0.011% of the general population [1], which indicates that the probability that an IA will rupture is approximately 1/181. Unfortunately, there are currently no accurate means to distinguish a rupture-prone aneurysm from those which would never rupture [1]. This presents a challenge for clinicians treating the disease in deciding whether treatment involving surgical intervention should be chosen. Aside from being costly, surgical treatment of aneurysms by itself imparts its own risks of 10% morbidity and 2.6% mortality [2] on the patient. An effective method of assessing whether an aneurysm will rupture would therefore be highly beneficial, in that costly and risky neurosurgery would then be performed only on the patients who require it for the prevention of inevitable SAH.

Perhaps the oldest criterion used for assessing the likelihood of an IA rupturing is IA size. It is assumed that as an aneurysm becomes larger, so too does its potential to rupture. However, this rather intuitive metric has proven to be somewhat unreliable. In a 20 year retrospective study

of 945 patients with aneurysms, 31.3% of aneurysms less than 3mm in size ruptured, while 28.1% of aneurysms greater than 25mm in size did not rupture [3]. Clearly, size is not the sole factor in determining the risk of rupture, nor does it provide any insight for explaining why the 68.7% of the aneurysms less than 3mm in size did not rupture over the ones that did rupture.

In seeking a more mechanistic explanation as to why aneurysms rupture, the effect of hemodynamic stresses on the endothelium has been considered. In the majority of the circulatory system where vascular geometry does not change abruptly in space, the endothelium is constantly exposed to a blood flow-induced shear stress within a physiological range of 0.4 – 7.0 Pa [4]; however, at bifurcations where vascular geometry does contain high spatial gradients, the endothelium experiences a much larger range of shear stresses which can change directionally in time. Since most cerebral aneurysms occur in these regions, it has been hypothesized that such aberrant levels of wall shear stress (WSS: the time averaged projection of the Cauchy stress vector on the lumen surface) from blood flow is a prominent factor in the initiation and further progression of IAs. More precisely, aberrant WSS is thought to be responsible for the degeneration of the endothelium – the inner-most layer of the artery exposed to and responsible for sensing the hemodynamic loading imparted by blood flow [1, 9, 16]. The degeneration of the endothelium then allows further damage to the inner-more layers of the artery wall, causing the formation and further growth of aneurysms. As the aneurysm becomes increasingly pathological, the blood flow becomes increasingly aberrant, and the degeneration and outward growth of the wall continues until the stress on the wall exceeds its yield stress, and the aneurysm ruptures. Due to the vortex nature of intra-aneurysmal flow, the aberrant WSS on aneurysm walls are typically found to be lower than that on vessel walls; this is particularly pronounced in the dome region [5]. Because IAs typically rupture in the dome region where WSS is below the

physiological level, it believed that low WSS is a promoter of wall degradation in aneurysms[1]. It was shown by in vitro experiments [6] that 9.7 % of cultured endothelial cells not exposed to hemodynamic loading underwent apoptosis, or programmed cell death, after a period of 10 days as opposed to the 0.2% of cultured endothelial cells which were exposed to hemodynamic loading. Pentimalli [7] also reported in a separate study that apoptosis has been associated with IA rupture. Because of evidence suggesting that low WSS in IAs bring about wall degradation which leads to rupture, it is reasonable to develop a metric which predicts the existence of low WSS in IAs.

In 1999, a new geometric-based metric was proposed over size to assess the risk of IA rupture that incorporates the mechanistic explanation of low WSS being driving factor responsible for wall degradation in IAs. Ujiie and collaborators conducted an in vivo experiment using rabbit models in which artificial bifurcation aneurysms were surgically created and positioned at the apex of the abdominal aorta – common iliac artery bifurcation [9]. The aim of the study was to explore the relationship between the characteristic geometry of aneurysms and the intra-aneurysmal blood flow structure. In particular, the study focused on identifying blood flow structures which produced regions of slow moving blood flow responsible for producing low WSS. Aneurysms of different sizes and shapes were produced and the resulting velocity fields were measured using Doppler ultrasound velocimetry. The study found that intra-aneurysmal flow structure could be categorized by two fundamental patterns: flows containing one circulation region (Type I flow), and flows containing a primary circulation region in

---

[1] In contrast, Cebral et al. have reported the existence of high WSS (>15 Pa) in IA domes from computational studies, hypothesizing that high WSS causes wall degeneration [8].

conjunction with a second, much slower moving circulation region in the dome of the aneurysm (Type II flow). The study concluded that aspect ratio (AR), the height of the aneurysm divided by the neck diameter of the aneurysm, was the characteristic parameter responsible for governing the flow type in the aneurysm (Type I vs. Type II). The study further concluded that an aneurysm with an AR less than or equal to 1.6 would contain a Type I flow structure, while an aneurysm with an AR greater than 1.6 would contain a type II flow structure. The significance in making this distinction in flow type is that the Type II flow contains a region of slow-moving blood near the dome which greatly reduces the hemodynamic loading on the wall to well below the physiological range. Having a Type II flow structure therefore, could be significantly more detrimental to the integrity of the aneurysm wall as opposed to having a Type I flow. The outcome of the study was the introduction of a new geometric risk factor, AR, which, unlike size, offered a mechanistic explanation of why IAs rupture which incorporated the effects of cell biology in conjunction with hemodynamics.

The degree to which the AR conjecture has succeeded in predicting rupture is inconclusive. In a paper subsequent to their initial findings regarding AR, Ujiie et al reported that in a retrospective study of 129 patients with ruptured aneurysms and 72 patients with unruptured aneurysms, the difference in AR between ruptured and unruptured aneurysms was found to be statistically significant [10]. The study reported that 80% of ruptured aneurysms showed an AR greater than 1.6, whereas almost 90% of the unruptured aneurysms showed an AR of less than 1.6. The study concluded that AR is a more reliable rupture predictor than size. In partial conflict to these results, a study conducted by Nader-Sepahi et al consisting of a pool of 75 patients with 75 ruptured and 107 unruptured aneurysms concluded that AR on its own is no more reliable of a rupture predictor than size [2]. The reliability of AR as a reliable rupture predictor was further

diminished by a retrospective study of 53 unruptured and 94 ruptured aneurysms by Beck et al. [11], which concluded that ruptured aneurysms have a lower AR than unruptured ones – the converse of the findings of Ujiie's study[2].

In 2005, Raghavan et al. [12] proposed a cohort of size and shape indices with the intent to correlate them with rupture. Size and shape indices are ratios of particular shape features of interest which define and quantify an aneurysm's intrinsic geometric characteristics. Essentially, the Raghavan study extended the work by Ujiie (only in the sense of defining more geometric metrics) by adding other shape metrics which were hypothesized to influence intra-aneurysmal flow structure, although no endeavor was undertaken to investigate flow structures experimentally or computationally in these cases. While none of the size indices were found to be statistically different between the ruptured and unruptured cases, five shape indices were found to be significantly different between the ruptured and unruptured aneurysms of the 27 patients studied. The study concluded that quantified shape is a more effective means of discriminating between ruptured and unruptured aneurysms than size; in particular, five shape metrics were found to be statistically different between the ruptured and unruptured groups; AR was among the five.

While the Raghavan study made no attempt to relate the shape metrics to flow structure or hemodynamics, the study's outcome could suppose the conjecture that hemodynamic loading does indeed influence rupture since it had found AR and four other shape metrics to be significant predictors of rupture, and one shape metric, AR, had previously been shown to influence flow structure. Furthermore if more than one shape parameter were statistically significant between the ruptured and unruptured cases, then more than one shape metric may be

---

[2] It is uncertain as to precisely how AR was defined in both studies. Therefore, a difference in definition could possibly have contributed to the difference in conclusions between the two studies.

responsible for controlling intra-aneurysmal flow dynamics. Namely, the characteristic geometry of an aneurysm may be under-defined by recruiting AR as the only shape metric to define it. This notion is a possible explanation of why AR studies have yielded inconsistent results. The in vivo Ujiie study which introduced AR made no mention of any attempts to control any other geometric metric thought to be responsible for promoting the detrimental hemodynamic conditions caused by Type II flow, nor did it investigate the possibility of the critical AR of 1.6 being dependent on another shape metric. In a computational study categorizing flow patterns in surgically created aneurysms in 51 rabbits, Zeng et al. [13] found that among the 51 cases, the critical AR was not a discrete value of 1.6 as reported in the Ujiie study, but rather, ranged between 1.8 and 2.2. These findings suggest that the critical AR of an aneurysm is indeed not a universal number; rather, it is dependent on one or more size or shape metrics, and furthermore, is possibly dependent on the aneurysm's location relative to its parent vasculature, as well as on the type of parent vasculature itself. As a result of this notion, a study which would attempt to correlate AR with risk of rupture may yield a false conclusion if the effects of other size or shape metrics were not properly filtered from the study. One may also expect the same problem to arise in any study attempting to correlate any one geometric metric with rupture. Furthermore, statistically-based studies attempting to correlate multiple geometric metrics have the weakness of not offering any mechanistic explanation for the linkage of each metric separately or as a group to intra-aneurysmal flow dynamics. To better correlate the risk of an aneurysm rupturing with AR or any size or shape metric, a more extensive and systematic method than previously employed was surmised to be needed.

In this work, we present a parametric study which employed computational fluid dynamics (CFD) on a parametrically reconstructed basilar bifurcation aneurysm that identifies

one aneurysmal size and one aneurysmal shape metric responsible for influencing the critical AR, and an additional aneurysmal shape parameter responsible for controlling the size of secondary aneurysmal vortices. The study identifies how each of the geometric metrics affects the intra-aneurysmal flow structures, and develops a multi-variable relationship which predicts the critical AR for a given set of geometric parameters; demonstrating that critical AR is not a constant, rather, it is a function multiple variables, and ultimately, neither AR nor any other geometric metric is sufficient on its own to describe the intra-aneurysmal flow structure. The study then demonstrates how the number of vortices affects the WSS distribution on the aneurysmal wall and discusses the significance in a clinical setting. Finally, the theory developed in the study was challenged in its ability to predict the number of vortices in 27 clinical computational models of bifurcation aneurysms. This validation study serves as an indication of the practicality of the theory developed in this work and its applicability to a clinical setting.

2.0   METHODS: PARAMETRIC MODELING OF VASCULATURE

The rationale behind the choice of utilizing a parametric modeling method to accomplish the aim of this work is explained as follows. The primary aim of this study was to identify and quantify the relationship between characteristic geometry and flow type in cerebral bifurcation aneurysms. To quantitatively describe the characteristic geometry, geometric metrics were defined. Each geometric metric consisted of ratios of dimensions such as height and maximum diameter which are instrumental in defining the surface of the aneurysm. The final form of each geometric metric, or parameter, was $\frac{A}{B}$, where both A and B are characteristic geometric dimensions. To develop a relationship between a characteristic parameter of particular interest, P, and flow structure, the following method was used. A reference model containing $P = P_0$ would be altered such that it would contain the parameter $P_0 + \Delta P_0$. Both computational models would then be solved numerically, and the difference in flow structure would be observed and quantified. The process would then be repeated with models over a large enough range of P such that the trend between P and flow type could be identified. If the effects of parameters other than P are to be filtered from the change in solutions between the models, then all other parameters of interest to the study must not be permitted to vary among any of the models pertinent to that particular study. A method of producing models which can enforce such requirements was therefore required. Data from three-dimensional rotational angiography (3DRA) used to produce computational models of vasculature consists of on the order of tens of thousands of points

which are used to define the lumen surface. There is no initial information regarding any relationship between the points. This notion, in conjunction with the cumbersomely high number of data points, renders the systematic manipulation of P and only P highly impractical at best. It is therefore desirable to implement a method by which the geometry is defined by a manageable number of attributes which can be systematically controlled, and for this reason, a parametric modeling method was implemented to create the computational models used in the study to satisfy the study's requirements.

The method though, must also be capable of reproducing the characteristic features of the original vasculature defined by a set of tens of thousands of points by using a number of attributes that is three orders of magnitude less than the number of original data points. A potential for the oversimplification of the geometry exists and must be must be avoided so that the flow field in the parametrically reconstructed model accurately represents the flow field in the original clinical model. The parametric modeling method employed in this work had been initially developed by Zakaria et al. [14] exclusively for arterial bifurcations, and has been expanded upon by Zeng et al. [15] to include aneurysm modeling. The method produces a parametric reproduction of a clinical model by first extracting the centerline of the clinical model. Circular cross sections which measure the best fit diameter of the vessel are then defined normal to the centerline on a number of locations appropriate for capturing the characteristic features of the original surface. The surface of the parametric model is then created by a swept blend of the circular cross-sections. The model parameters which define the lumen surface for both the original model and its parametric reconstruction are compared in Figure 2.1. It is evident by comparing the two methods in Figure 2.1 that one can much more easily and effectively control the characteristic parameters of the aneurysm simply by adjusting the values

of the circular cross-sections defining the swept blend, or by adjusting the coordinates of the circular cross-sections' origins which define the centerline as opposed to manipulating the point cloud defining the original model. The adjustments mentioned would produce a wider versus a narrower aneurysm, or would produce a longer versus a shorter aneurysm respectively. The method could also be extended for use of manipulating parent vasculature, though this study focused exclusively on the effects of manipulating aneurysmal geometry.
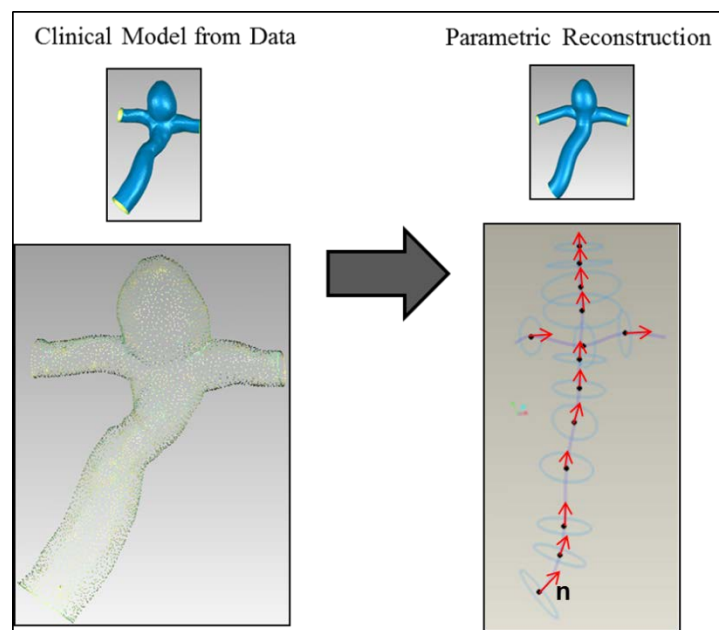
Figure 2.1. Comparison between clinical model and parametric model

The parametric modeling method's ability to recreate both the flow structure and the WSS distribution is shown in Figures. 2.2 and 2.3. Referring to Figure 2.2, it is evident that the same flow structure (a single vortex flow) is produced by both the parametric and clinical models. The spatial distribution of the velocity magnitudes are similar, as is the vortex core positioning with respect to the aneurysm. The WSS contours shown in Figure 2.3 provide a more quantitative comparison of the velocity fields from which the WSS distribution is

10

produced. The graph in Figure 2.3 displays the WSS values along an arc on the aneurysm wall; beginning where the incoming flow impinges on the neck and ending where the flow exits the aneurysm tangent to the neck (refer to the diagram in Figure 2.3 for visual aid). It is seen that all qualitative features of the WSS along the arc are captured. The WSS at the point of impingement on the neck is markedly high. As one moves along the arc into the dome region, the WSS drops in magnitude, then progressing further along the arc, the WSS magnitude increases as the flow exits the aneurysm. Furthermore, the magnitudes between the two models are in good agreement with each other in the three distinctive regions.
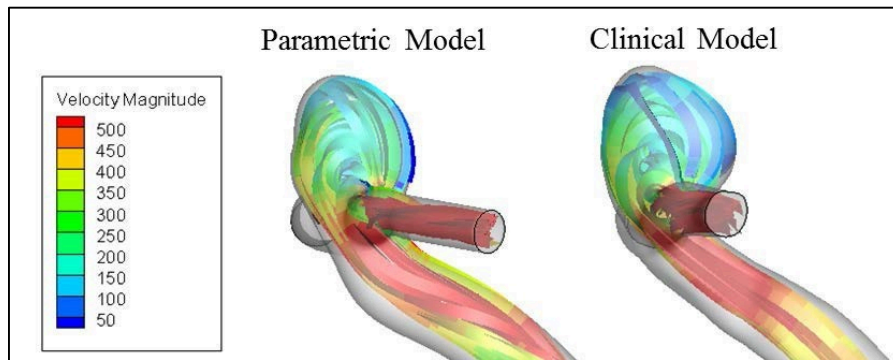
Figure 2.2. Comparison between parametric model and clinical model streamlines at systole
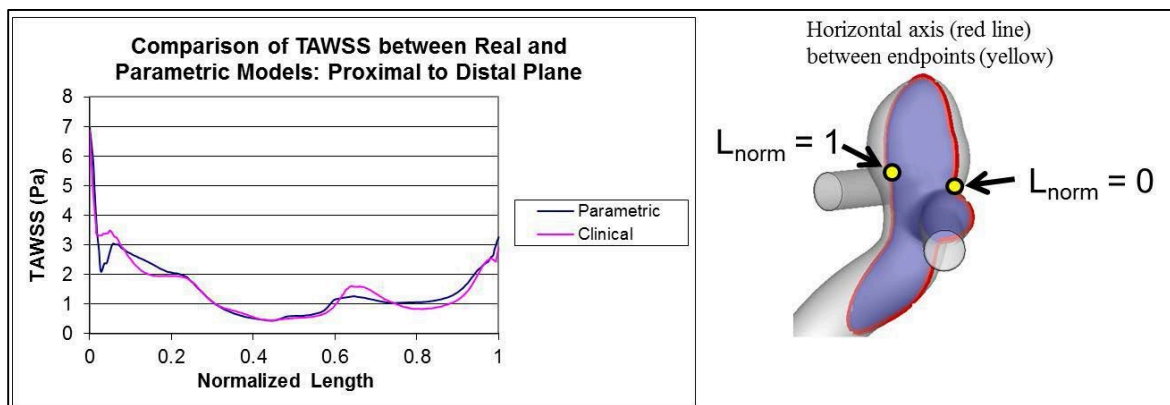
Figure 2.3. Comparison between parametric model and clinical model WSS

The main strength of this parametric method is the ability to produce a family of models in which a particular parameter of interest is varied in controllable increments while fixing all other parameters of interest while closely reproducing a clinically relevant flow field. For example, for the original in vivo Ujiie study of aspect ratio, one could in principle implement the parametric method to produce computational models of a family of aneurysms with identical parent vasculature but with different ARs. All other characteristic geometric features of the aneurysms could have been kept identical such that the result would be a family of aneurysms varying by AR alone. The only variation among the family of models would be a progressive stretching of the aneurysm in the direction normal to the neck from one model to the next (in other words, a progressive variation of AR); therefore, the pure effects of increasing AR could be observed, untainted by the confounding effects of any other covariant. A critical AR could then be accurately established based on the fixed values of the other geometric parameters. It would then be possible to investigate whether the same determined critical AR would hold true for different values of the previously fixed parameters. A visual demonstration of increasing AR is shown if Figure 2.4.
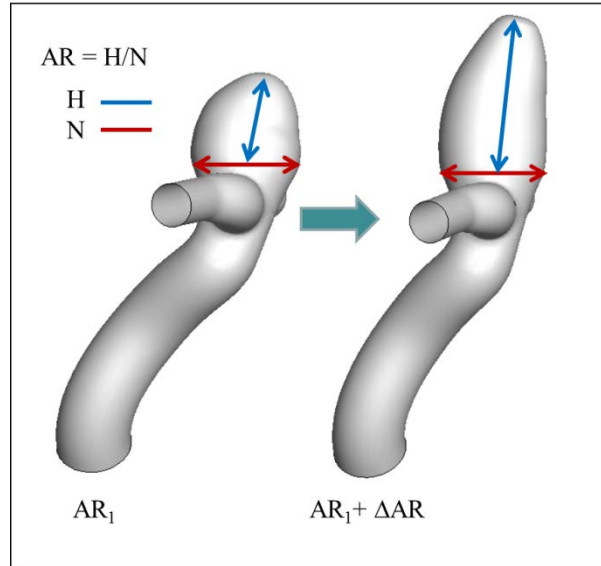
Figure 2.4. Example of modifying a parameter of interest

Figure 2.4 demonstrates the concept upon which the parametric study in this work is built. By varying parameters by the method shown in Figure 2.4 and comparing the calculated flow fields, we were able to isolate the change in the intra-aneurysmal flow to a single parameter and quantify the change. This method, as opposed to using clinical data, is advantageous for the scope of our work, in that precise control over the parameters is permitted, whereas with using clinical data, obtaining many cases containing the exact desired geometry is nearly impossible. The work presented in the next section utilized the advantages of parametric modeling to determine how each parameter affects intra-aneurysmal flow structure.

3.0 ANEURYSMAL GEOMETRIC PARAMETERS AND FLOW STRUCTURE:

SINGLE VARIABLE STUDIES

3.1 DEFINITION OF CHARACTERISTIC GEOMETRIC PARAMETERS

In order to develop a relationship between characteristic aneurysmal geometry and intra-aneurysmal flow structure, it was first necessary to define characteristic geometric parameters which are responsible for determining whether the intra-aneurysmal flow is Type I or Type II. Ujiie et al. demonstrated the existence of a critical AR which divides the set of all bifurcation aneurysms between having Type I or Type II flow [9]. Whether or not AR is a reliable predictor of aneurysmal rupture has since been the subject of much study; the format of the CFD parametric study of this work was therefore based on determining a critical AR for each case being studied. Because, evidence in the literature has suggested that critical AR is not a universal constant, other characteristic parameters were recruited into the parametric study of this work to determine what relationship, if any, exists between other characteristic parameters and critical AR. Three characteristic parameters hypothesized to influence critical AR were incorporated into the parametric study: Bottle Neck Factor (BF) (W/N), Conicity Parameter (CP) (S/H), and Size Index (SI) (P/N), and are diagramed in Figure 3.1.
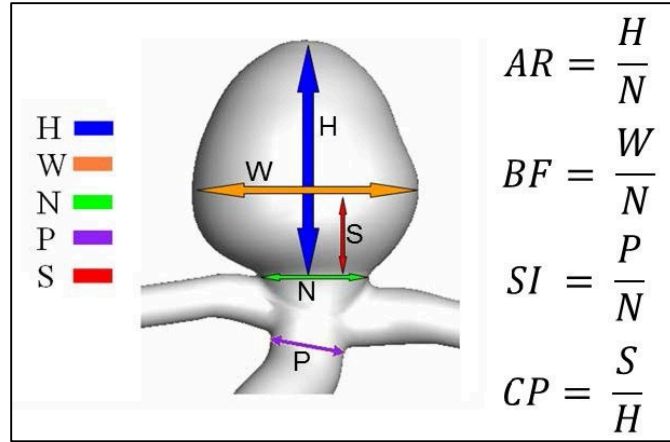
Figure 3.1. Geometric characteristic parameters with respect to geometry

As seen in Figure 3.1, the selected dimensional parameters H, W, N, and S are instrumental in defining the characteristic shape of the aneurysm, while P is instrumental in defining the size of the parent vasculature. For all models in the parametric study, the parent vasculature remained identical. Every parametric aneurysm in the study was thus defined by (H/N), (W/N), (P/N), and (S/H), and all other parameters which could be potentially be defined were neglected, as they were assumed to have an insignificant impact on defining the intra-aneurysmal flow dynamics. By modifying (H/N), (W/N), (P/N), and (S/H), all geometries in the parametric models in the study were produced from one original reference model of a bifurcation aneurysm located on the tip of the basilar artery, while the parent geometries in all parametric models were kept identical in all aspects. Figure 3.2 demonstrates examples of three aneurysms, all having different shapes, which all stem from the same original reference model.
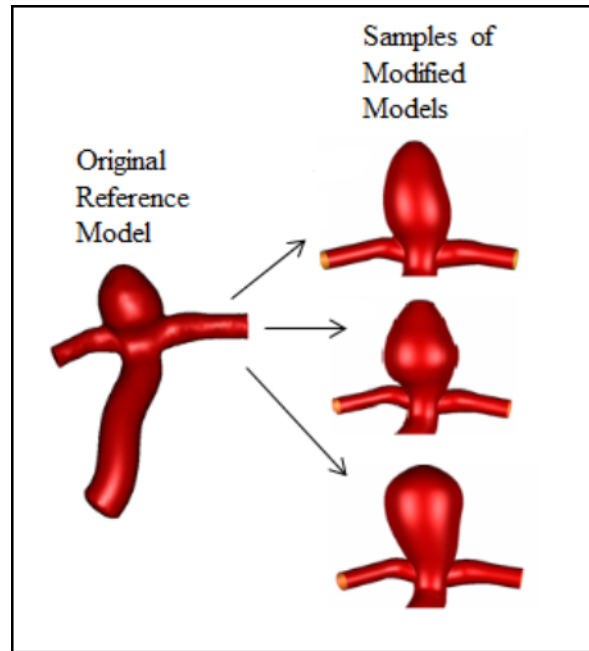
Figure 3.2. Demonstration of the notion that all parametric models originated from one reference model

A description of each parameter used in the parametric study is given in the following subsections. Refer to Figure 3.3 for visual detail regarding how each parameter affects the aneurysmal geometry.

3.1.1 Description of Aspect Ratio

The aspect ratio, (H/N), is defined by the height of the aneurysm measured from the center of the neck plane to the center of the dome of the aneurysm. In the reference model of this study, the arc length of the centerline is within 10% of the linear distance defined by H; therefore, the distance H is trivially approximated by a straight line. The neck diameter, N, is defined as the diameter of the neck plane. The neck plane is defined by the minimal diameter cross-section normal to the centerline of the geometry in the region where the aneurysm is joined to the

bifurcation. In terms of distance on the centerline, this region is typically small and both well and trivially defined as a result. Aspect Ratio is bounded between zero and infinity: as AR becomes larger; the aneurysm is stretched in the direction normal to the neck, and becomes more elliptic in shape with the centerline axis being the long axis. In human aneurysms, AR has been found to range from $0.60 - 5.53$ [16]. Several means and standard deviations of AR have been reported. Here, we present the following: 1.86 ± 0.86; ruptured 1.85 ± 0.79, unruptured 1.27 ± 0.40 [16].

3.1.2   Description of Bottle-Neck Factor

The bottleneck factor, (W/N), is defined by the maximum cross-sectional diameter in the aneurysm divided by the neck cross-sectional diameter. Bottleneck factor is bounded between one and infinity. A BF of one indicates that the neck cross-section is also the widest cross-section in the aneurysm, and W therefore equals N. As BF tends toward to infinity, the aneurysm sidewalls balloon outward, shaping the aneurysm more elliptically in the axis perpendicular to the centerline. In human aneurysms, BF has been shown to range from 1.0 to 6.35 with a mean and standard deviation of 1.91 ± 0.86 [16].

3.1.3   Description of Size Index

The size index, (P/N), is defined by the neck cross-section divided by the cross section of the parent artery where the bifurcation region initiates (see Figure. 3.1). This parameter was used to

quantify the length scale (size) of the aneurysm to the length scale (size) of the parent vessel. Since P was held constant in all parametric models, altering N was the only means of varying (P/N). To maintain a scaled, consistent aneurysm shape, H, W, and S were scaled accordingly to changes in N in order to keep the same characteristic aneurysmal shape. Size index is bounded by 0 and infinity. A small size index indicates that the parent vessel diameter is small in comparison to the aneurysm neck size; the aneurysm is therefore large with respect to the parent vessel. A large size index indicates that the parent vessel is much larger than the aneurysm neck, and that the aneurysm is small in comparison to the parent vessel. With a mean basilar artery diameter of 3.32 mm and a reported range of neck sizes of 1.1mm-12.9 mm, an estimated range of SI is between 0.25 - 3.0 [16].

3.1.4   Description of Conicity Parameter

The Conicity Parameter, (S/H), indicates the location of W, the maximum cross-sectional diameter in the aneurysm, with respect to the vertical axis of the aneurysm. The Conicity Parameter is therefore bounded between 0 and 1: a CP of 0 indicates that W is also N, meaning that the widest section of the aneurysm is at the bottom of the aneurysm (the neck). In contrast, a CP near 1indicates that W is near the dome of the aneurysm. The mean and standard deviation of CP are: ruptured 0.35 ± 0.22; unruptured ruptured 0.30 ± 0.19 [12].
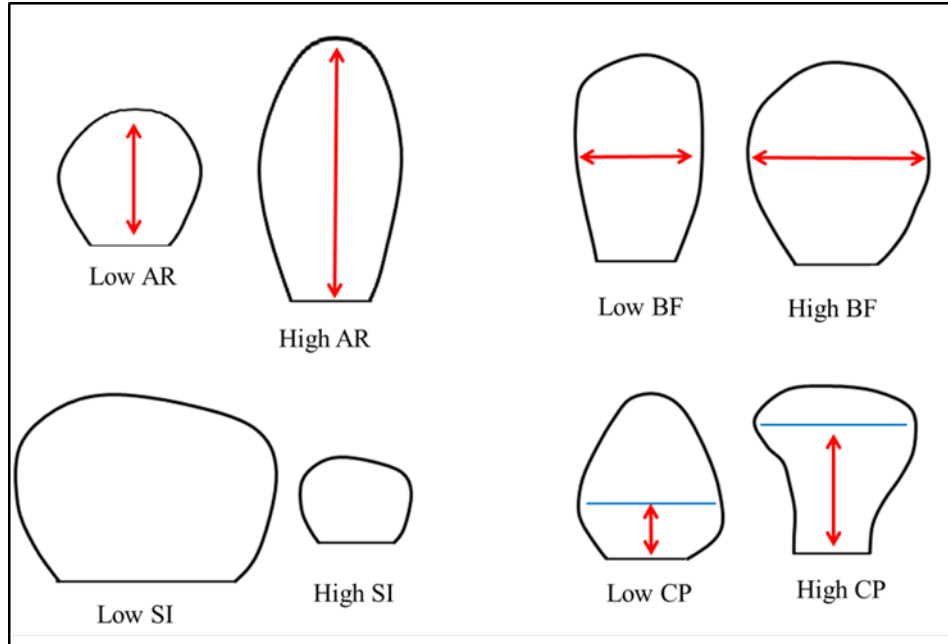
Figure 3.3. Role of characteristic parameters in controlling aneurysmal shape

3.2 NUMERICAL MODELING AND BOUNDARY CONDITIONS

All models used in the studies in this work, whether parametric or clinical, are computational models whose flow fields governed by the Navier-Stokes equation were approximated via CFD using the finite element method implemented in the commercial software Adina (Adina R&D, Watertown, Mass.). The blood was modeled as an isothermal, incompressible, Newtonian fluid with a density of 1050 kg/m^3 and a viscosity of 0.0035 Pa s. All models were meshed with a hexahedral mesh grid varying between 30,000-35,000 elements, depending on the size of the aneurysm. The number of elements was based off the premise that the average change in WSS was less than 10% between the 35,000 element grid and a 60,000 element grid – the maximum amount of elements which the work station (Dell Precision 890, dual core 3.0 MHz, 4GB RAM)

19

on which the simulations were conducted could accommodate. The wall of the vasculature was modeled as rigid and the velocity vector was imposed as identically zero on the wall. A time varying parabolic velocity boundary condition was applied at the inlet of the basilar artery. A modified traction boundary condition was applied at the outlet of one of the two daughter branches; the outlet velocity of the other daughter branch was imposed such that the WSS magnitude at both daughter branch outlets was equal[3]. The locations of the boundary conditions on the model are diagramed in Figure 3.4; the waveform used in the study is shown in the same figure. A temporal resolution study demonstrated that a time step of 0.02s was sufficient for properly resolving the solution in time when using the 35,000 element mesh grid since no qualitative differences existed in the flow field during systole and diastole between time steps of 0.02s and 0.01s, and that differences in WSS between using 0.02s and 0.01s time steps were less than 1%.

Γ_1	Γ_2	Γ_3
$v = v(r,t)\, n_{\Gamma_1}$ $v(0, t_{systole}) = 800\, \dfrac{mm}{s}$	$t' = T' \cdot n = Cn;$ $T' = -pI + \mu \nabla v$	$v = v(r,t)\, n_{\Gamma_3}$ v is chosen such that: $\tau_2 = \tau_3 \qquad q_2 + q_3 = -q_1$ $q_i = q_i n_i$
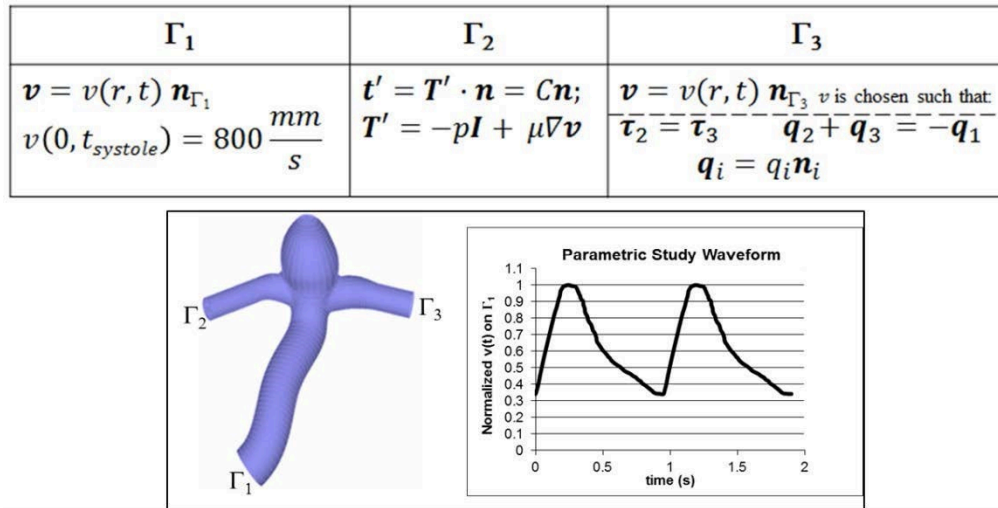
Figure 3.4. Hexahedral mesh grid with boundary conditions for the reference model

---

[3] Boundary condition sensitivity studies indicated that the flow field is largely insensitive to the choice of daughter branch for applying the modified traction boundary condition

In order to determine whether the selected characteristic parameters (H∕N), (W∕N), (P∕N), and (S∕H) have an impact on Type I versus Type II flow in aneurysms, a single variable parametric analysis was performed for each characteristic parameter. For each single variable analysis, a family of parametric models was created such that only the characteristic parameter permitted to vary amongst the family was the characteristic parameter of interest to that particular study while the other characteristic parameters were held fixed. By this methodology, it was possible to identify how each parameter affected the critical AR and flow structure of the bifurcation aneurysm.

3.3   IDENTIFICATION OF CRITICAL ASPECT RATIO

The critical AR study began with the production of a family of models containing the reference (W/N), (P/N), and (S/H) parameters of the original reference model, while (H/N) was varied between 0.9 and 2.3 (Table 3.1). The solutions to the models were then obtained. Among this group, the critical AR was determined to be 1.3, where the models with AR of 1.4 and above all exhibited Type II flow, and the models 1.3 and below exhibited Type I flow. In the models containing Type II flow, the primary vortex was observed to remain nearly constant in size, while the secondary vortex enlarged progressively with increasing AR to occupy the progressively increasing volume of the dome region (Fig 3.5). The intra-aneurysmal volumetric flow rates were found to decrease by 6.5 % over the AR range from 1193 mm^3/s with AR = 0.9 to 1113 mm^3/s with AR = 2.3 (Figure 3.6). This behavior in volumetric flow rate indicates that as the aneurysm's volume increases (with increasing AR) there is no compensating increase in

blood flow to the aneurysm. Such a notion suggests that, in conjunction with the fact that the primary faster-moving vortex does not change in size with increasing AR, as AR increases, so too do conditions in the dome for localized blood stagnation and thrombosis which are thought lead to the localized degradation of the chemical structure of the wall [9]. The AR trends of mildly diminished flow rate and increasing volume for the secondary vortex to occupy were found to be monotonic; this suggests that an aneurysm with a progressively increasing AR will necessarily experience an increase in the size of the region of slow moving flow near the dome, provided that all other parameters remain fixed.
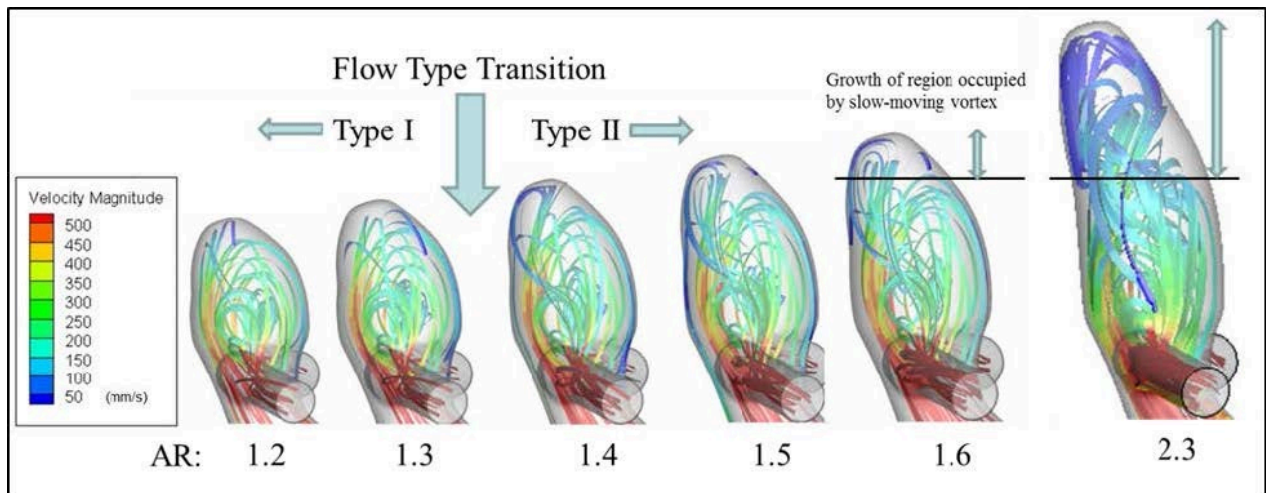
Figure 3.5. Flow type trend with increasing AR

Table 3.1. AR study model parameters

Parameters for AR Study			
H/N	W/N	P/N	S/H
0.9 - 2.3: 0.1	1.0	0.67	0.33

22
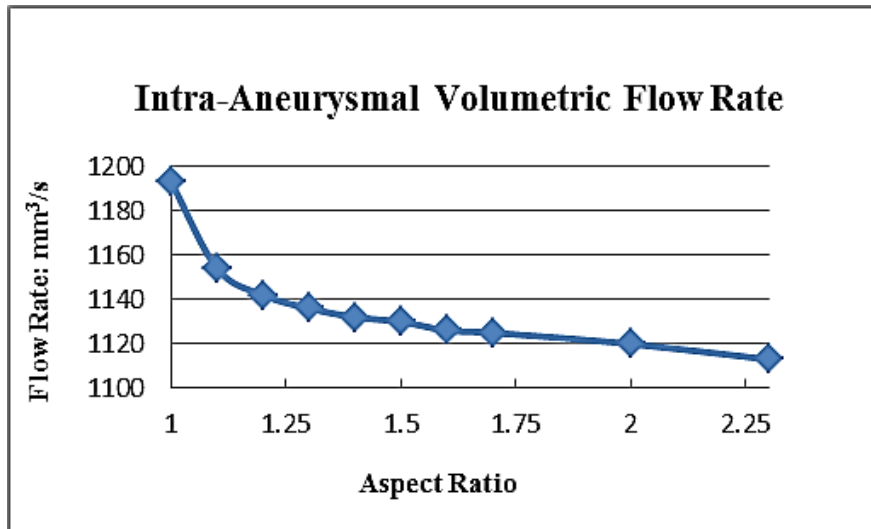
Figure 3.6. Intra-aneurysmal flow rate with increasing AR

3.4 THE RELATIONSHIP BETWEEN CRITICAL ASPECT RATIO AND BOTTLE-NECK FACTOR

The BF study began with the production of a family of models beginning with the model with an AR of 2.0 in the critical AR study family of models (Table 3.2). This model with two intra-aneurysmal vortices was used as the reference model for the BF study. The reference model had a BF of 1.0, indicating in conjunction with its AR, a rather tubular shaped aneurysm. Four parametric models were created which increased the BF of the BF study reference model to a maximum of 2.0 in approximate increments of 0.25. The goal of the study was to investigate whether or not a change in flow structure from Type II to Type I would result from increasing the BF of the reference model containing a Type II flow. It was found that as BF was increased, the flow structure transitioned from Type II to Type I for a BF of 1.25 (Fig 3.7). These results

23

thus demonstrated that critical AR is indeed dependent on other characteristic parameters as opposed to being a constant. Furthermore, the transition between Type II to Type I flow occurred at an AR of 2.0 as opposed to an AR of 1.3 in the AR study. In a study of saccular aneurysm geometry, Parlea et al. reported the average AR amongst a set of 87 simple-lobed aneurysms to be 1.86 [18]; this average falls within the upper and lower bounds of the critical AR range determined heretofore. This notion suggests that for most aneurysms, using a single value of critical AR to define intra-aneurysmal flow structure can result in an incorrect prediction of flow type since the average AR falls within the large range thus far found of possible critical AR.

Aside from influencing flow type, it was also found that BF controlled the degree to which the vortex was able to enter the aneurysm: as BF was increased, the degree to which the vortex occupied the aneurysm also increased. As W approached H (the aneurysm became increasingly spherical in shape), the center of the Type I flow structure approached the center of the aneurysm. This is in contrast to the model with a BF of 1.0, where the center of the primary vortex of the Type II flow structure was positioned near the neck region, allowing more volume in the upper half of the aneurysm for the existence of the secondary vortex (refer to Figure 3.7). Therefore, a possible physical explanation for the role of BF in determining the intra-aneurysmal flow structure is that there is a maximum degree to which the streamlines of a vortex for any instant in this physical situation can possess an elliptic shape before the circulation region must split into two regions in order to form two vortices with streamline patterns closer to being circular.
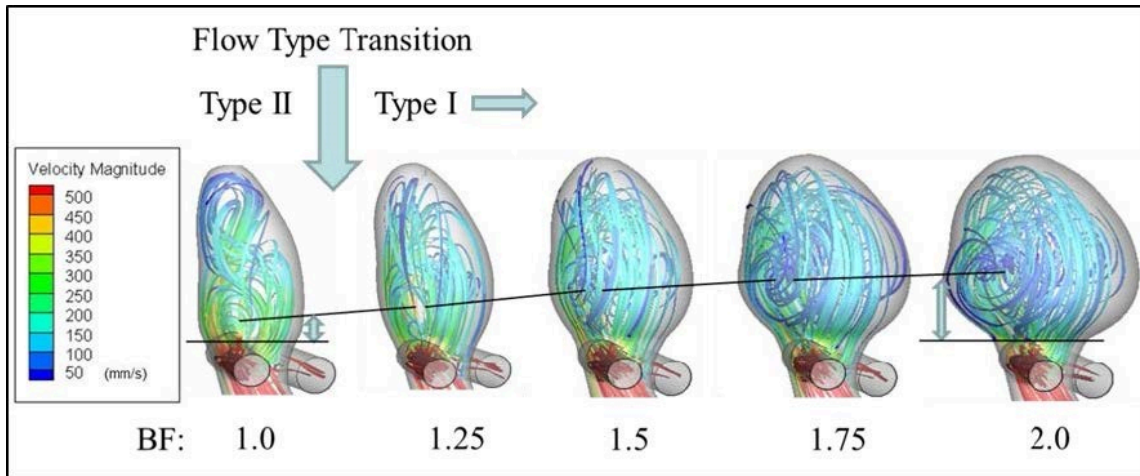
Figure 3.7. Flow type trend with increasing BF

Table 3.2. BF study parameters

Parameters for BF Study			
H/N	W/N	P/N	S/H
2.00	1.0-2.0: 0.25	0.67	0.33
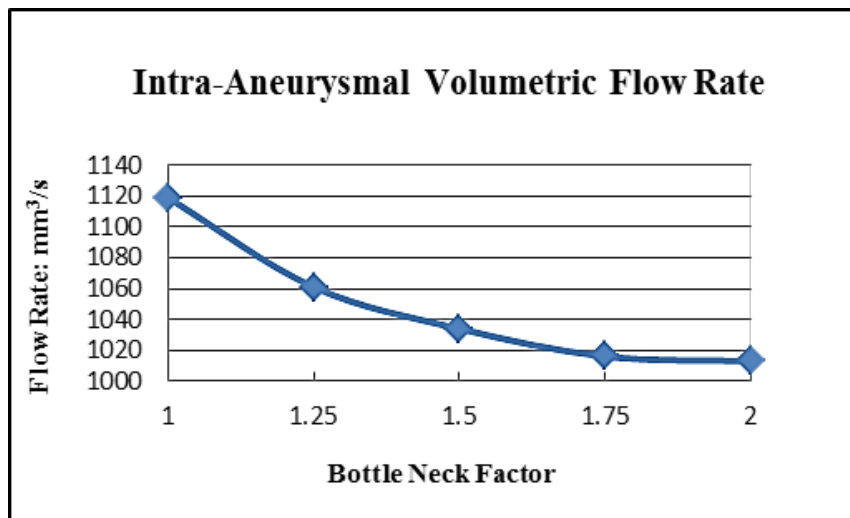
Figure 3.8. Intra-aneurysmal flow rate with increasing BF

3.5   THE RELATIONSHIP BETWEEN CRITICAL ASPECT RATIO AND SIZE INDEX

The SI study began by using the original reference model to produce a family of models in which SI ranged from 2.0 to 0.33 (Table 3.3). In this set of models, the aneurysm shape remained unchanged while the length scale of the aneurysm with respect to the parent geometry was varied. When the SI of the original reference model was greater than or equal to 1.33, the flow type transitioned from Type I to Type II, in a manner similar to that observed in the BF study (Figure 3.9). As the Type I flow aneurysms became smaller, the degree to which the single vortex occupied the aneurysm became progressive less; the vortex location shifted from being centered in the aneurysm to being centered below the neck region and into the parent geometry bifurcation region. As the aneurysm became increasingly smaller, the degree to which the single vortex occupied the aneurysm diminished to the extent that a slow moving secondary vortex began to fill the void in the dome left by the departing primary vortex. The neck diameter of the smallest aneurysm in the SI study was half of the parent vessel diameter, indicating a small aneurysm. Furthermore, the AR was a low 1.1, below the previously established lower critical AR of 1.3; this aneurysm however did possess a slow moving secondary vortex because the small neck relative to the parent vessel acted as a constrictive mechanism which prevented flow from sufficiently entering the aneurysm. The primary vortex in this case existed primarily outside the aneurysm. This mechanism could offer insight as to why IA size alone has been shown to be an unreliable predictor of rupture, particularly in the cases of small aneurysms

rupturing despite them being thought of as having a negligible risk of rupturing. Furthermore, the

SI study demonstrated that SI is yet another characteristic parameter which is instrumental in

determining the intra-aneurysmal flow structure with respect to flow type.
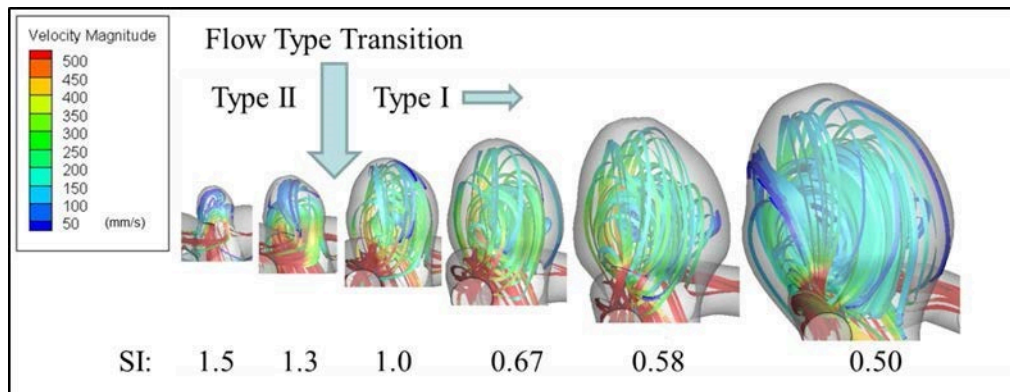
Figure 3.9. Flow type trend with increasing SI

Table 3.3. SI study parameters

Parameters for SI_1 Study			
H/N	W/N	P/N	S/H
1.1	1.0	2.0 - 0.33	0.33
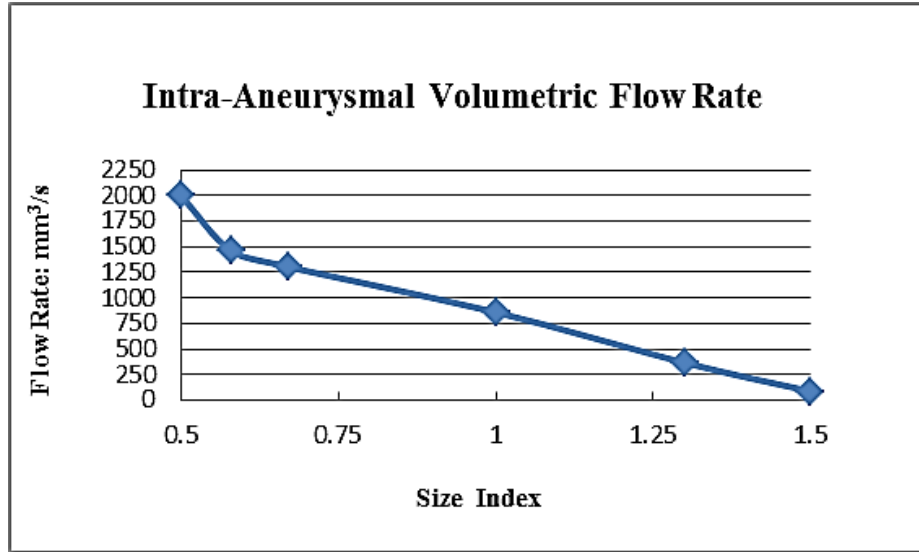
Figure 3.10. Intra-aneurysmal flow rate with increasing SI

To further explore the behavior of the phenomenon of intra-aneurysmal flow constriction in small aneurysms, the same SI test was repeated except that the models in the second SI test were given a high AR, ensuring the flow was well within the Type II category (Table 3.4). The results of the second SI study indicate that for Type II flow, there is an optimal SI which maximizes the blood velocity at the dome; in this particular study, the optimal SI was 0.67. As SI decreases below the optimal SI, the ratio between the sizes of the two vortices remains constant; however, the velocity near the dome decreases. As SI increases, the ratio between the size of the secondary vortex and the size of the primary vortex increases as the primary vortex becomes increasingly absent from the aneurysm. The region of low velocity near the dome also grows with increasing SI as shown the systolic streamline plots (Figure 3.11). The phenomena observed in the second SI study produces insight as to possibly why small aneurysms rupture like the first SI study – that the relatively small neck size acts as a means of constricting flow into the aneurysm (particularly to the dome region), leading to conditions detrimental to the wall.

28
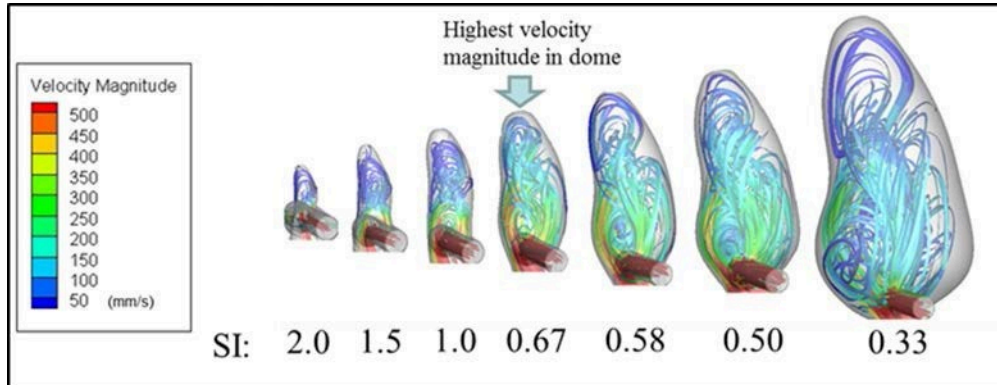
Figure 3.11. Flow type trend with increasing SI for exclusively Type II flows

Table 3.4. Parameters for exclusively Type II SI study

Parameters for SI_2 Study			
H/N	W/N	P/N	S/H
2.2	1.0	2.0 - 0.33	0.33

3.6   FLOWTYPE AND CONICITY PARAMETER

To be meaningful, the CP study had to be performed using a reference model with a significant BF, since, as BF approaches 1.0 from above, CP's effects become increasingly diminished (and CP is meaningless for BF = 1.0). Therefore, the CP reference model was chosen to have a BF of 1.5 and a Type I flow structure. In the CP study, CP was varied from 0.25 to 0.75. The results showed that CP had no influence on the flow type, in that the Type I flow structure was not

transitioned to a Type II flow structure for any value of CP. In a second CP study with cases produced from a reference model with Type II flow; there was no change in flow type in the set like with the exclusively Type I. It was therefore concluded that varying CP will not cause a change in flow type. The parameters of the studies are listed in Tables 3.5 and 3.6.

While CP did not influence flow type for both Type I and Type II flows, it did have a significant qualitative effect on the two flow types. For Type I flows, increasing CP had the effect of shifting the vortex higher into the aneurysm (Figure 3.12). For Type II flows, increasing CP significantly changed the ratio of the sizes between the primary and secondary vortices. For a CP of 0.25, the division between the two vortices occurred at approximately $2H/3$; whereas for a CP of 0.75, the vortex division occurred at approximately $H/4$, leading to a nearly 500% increase in volume for the slow moving secondary vortex to exist (Figure 3.13). The Conicity Parameter can therefore be categorized as a parameter that qualitatively influences the particular flow type found in an aneurysm as opposed to quantitatively affecting the flow category (Type I versus Type II).
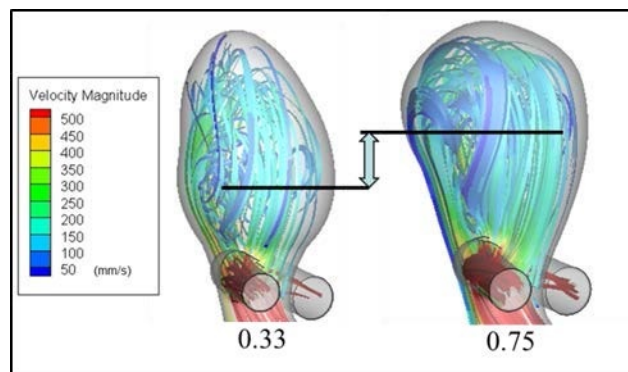
Figure 3.12. Flow trend with increasing CP for exclusively Type I flows
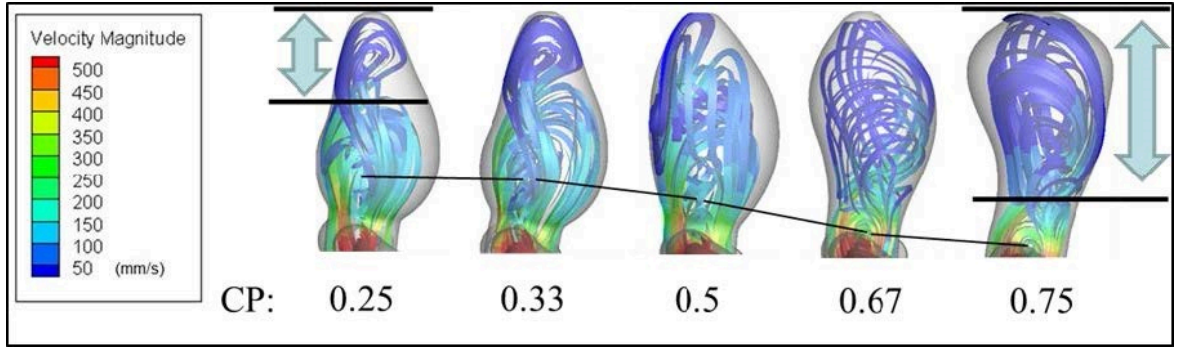
Figure 3.13. Flow trend with increasing CP for exclusively Type II flows

Table 3.5. Parameters for Type I CP Study

Parameters for CP_1 Study			
H/N	W/N	P/N	S/H
2.0	1.5	0.67	0.25-0.75

Table 3.6. Parameters for Type II CP Study

Parameters for CP_2 Study			
H/N	W/N	P/N	S/H
2.2	1.5	1.00	0.25-0.75

3.7   DISCUSSION

The single parameter study demonstrated two important concepts. First, the study clearly demonstrated the complexity of the mechanisms responsible for determining the type of intra-aneurysmal flow relative to what has been proposed previously. Flow type is not simply defined

31

by a single characteristic parameter, but rather by multiple parameters acting in conjunction with each other. Second, the study demonstrated how the severity of slow moving flow near the dome region can range amongst Type II flows and that slow moving flow can even be brought about in Type I flows. Moreover, this variation in slow moving flow severity was shown to not only be controlled by AR, but by all of the other characteristic parameters studied. The two concepts developed by the single parameter study should offer insight as to possibly why AR alone failed to be a sufficient predictor of rupture in practice: AR alone is insufficient information to determine the flow conditions within a bifurcation aneurysm. Therefore, AR (or any other parameter) on its own cannot be expected to yield consistent conclusions with respect to rupture.

Furthermore, the single parameter study yielded an unanticipated result: it provided insight as to possibly why small aneurysms rupture. The SI study clearly demonstrated that adequate blood fails reach the domes of aneurysms with small openings relative to the cross-sectional area of the parent vessels. As a result of the inadequate blood flow, the WSS in the dome region becomes detrimentally low. The small neck region provides substantial resistance to the inflow such that the fast-moving circulation region exists primarily in the bifurcation region as opposed to within the aneurysm. As a result, the same slow-moving flow conditions found in large bifurcation IAs with high ARs can exist in small IAs with small ARs and BFs.

3.8   CONCLUSION

The single parameter studies importantly identified three parameters which are responsible for influencing critical AR and flow structure. The trends of the effects these parameters have on the

two different flow types were also demonstrated. The single parameter study however did not offer any complete, quantitative method to determine critical AR for a general case. Critical AR had been calculated over a range of 1.1 among the different single variable studies (more than half the average AR reported by Parlea), yet, no relationship among critical AR, BF, and SI was established. The need for a multivariable study of AR, BF, and SI which can clearly define critical AR as a function of BF and SI for any given CP should therefore be recognized.

4.0 ANEURYSMAL GEOMETRIC PARMETERS AND FLOW STRUCTURE: MULTIVARIABLE STUDY

4.1 IDENTIFYING CRITICAL ASPECT RATIO AS A FUNCTION OF MULTIPLE PARAMETERS

The work presented in the previous chapter focused on developing the relationship between AR, BF, SI, CP, and critical AR. Relationships between each parameter and critical AR were established; however, critical AR was found to range between 0.9 and 2.0 amongst the single variable studies. The existence of such a large range of critical AR implies that critical AR is a function of multiple variables. Building on the work described in Chapter 3, the work presented in this study was conducted to determine a function which predicts critical AR - the AR for which intra-aneurysmal flow transitions between Type I and Type II flows - as a function of BF and SI. The methodology for the multi variable critical AR study was as follows. For all models in this study, CP was held constant at 0.33 (its value in the original reference model), as it was previously determined to have no effect on controlling the flow type of a bifurcation aneurysm. Upon establishing the CP criterion, a family of parametric models with a constant SI was then considered. In the constant SI family, four different models (each having a different BF) were created to produce the reference models of four sub-families. Then, from each reference model in the BF sub-families, AR was varied among a range wide enough to capture the transition

between Type I and Type II flow. The entire BF sub-family process was then conducted for two other SI families. The result was the production of three SI families (SI = 0.67, 1.0, and 2.0), each with four BF sub-families, where a critical AR as a function of BF and SI was determined for each model in each BF sub-family, all with a CP of 0.33. CFD studies were then performed on all models to obtain the approximated flow fields.

When completed, the results of the studies on all three SI families yielded a nearly linear relationship between critical AR and BF for $1.3 < AR_{critical} < 4$ and $1 < BF < 2.5$. Using the least-squares regression method, the minimum r^2 value for the AR-BF relationship amongst the three SI families was 0.97 when fitted to a linear model. It was furthermore found that the AR-BF slope among the three SI families was nearly identical within the almost linear region. Among the SI families, it was found that a logarithmic term best fit the relationship amongst the three SI families ($r^2 = 0.96$). The multi-variable study finally yielded function

$$AR_{critical} = 2.5\,\frac{W}{N} - 0.92\ln\frac{P}{N} - 1.5$$

which describes critical AR as a function of BF and SI for a given CP (Figure 4.1).
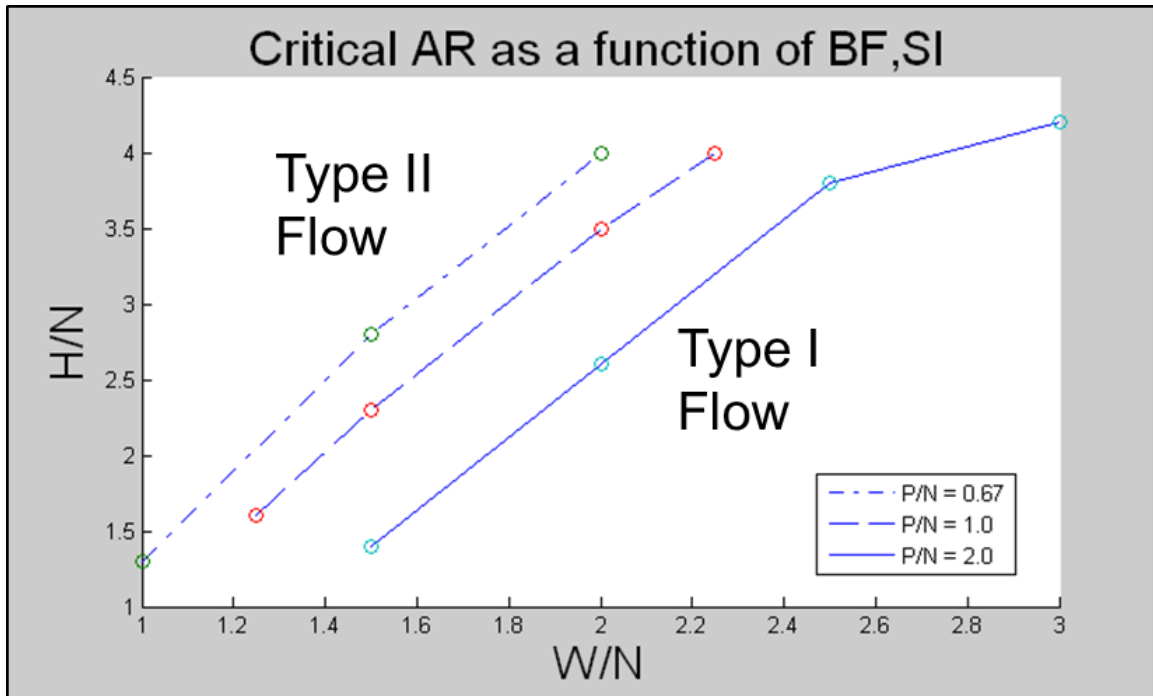
Figure 4.1. Graphical representation of critical AR equation

Figure 4.1 demonstrates the futility of attempting to define critical AR as a universal constant. The flow type region is divided between Type I and Type II a line in the AR-BF plane depending on the value of SI. For a given SI, if the aneurysm possesses an AR-BF point to the upper left of the SI line, then the flow-type is type II, if the AR-BF point is on the opposite side of the SI line, the flow is Type I. Flows very near to or on the SI line indicate the onset of flow type transition. Referring the streamlines in the AR study section of Chapter 3, it can be seen that the difference of velocity magnitude reduction in the streamlines near the dome, as well as the size of this secondary-vortex region, is not profound between the AR cases of 1.3 and 1.4, and even less so once the transition mark has been passed from 1.4 to 1.5. Therefore, the severity of the Type II flow case should be judged by how far above and to the left of the respective SI line the AR-BF point lies as opposed to simply considering all points in the entire Type II region as being equally severe.

The critical AR equation has valuable potential: it can offer clinicians a tool for assessing the hemodynamic conditions present in a bifurcation aneurysm by utilizing geometric measurements obtainable from angiography. Furthermore, the proposed critical AR equation method offers a far more complete description of the hemodynamics present in the aneurysm than would AR alone, because the developed method takes into consideration the other characteristic parameters shown to have important influence on the intra-aneurysmal flow type.

4.2   SENSITIVITY OF MULTI-VARIABLE CRITICAL ASPECT RATIO CONCLUSION TO REYNOLDS NUMBER

The results of the full multi-variable study summarized in Figure 4.1 which complete the flow type prediction theory in this work seem quite extensive and promising. However, it is reasonable to question the sensitivity of the critical AR equation to parent artery Reynolds number (Re). Therefore, numerical studies were conducted to determine whether the obtained critical AR equation is valid over a practical range of Reynolds numbers. In the parametric studies, the systolic Re defined in the basilar artery was approximately 500. A typical range of Re for the circle of Willis is 300-800 [9]. It was therefore decided that the maximum deviation for the original Re would be by ±40%. The AR study (Fig 3.4, Table 3.1) was repeated at Reynolds numbers of ±20% and ±40% near the previously calculated transition range. The results are displayed in Fig 4.2.
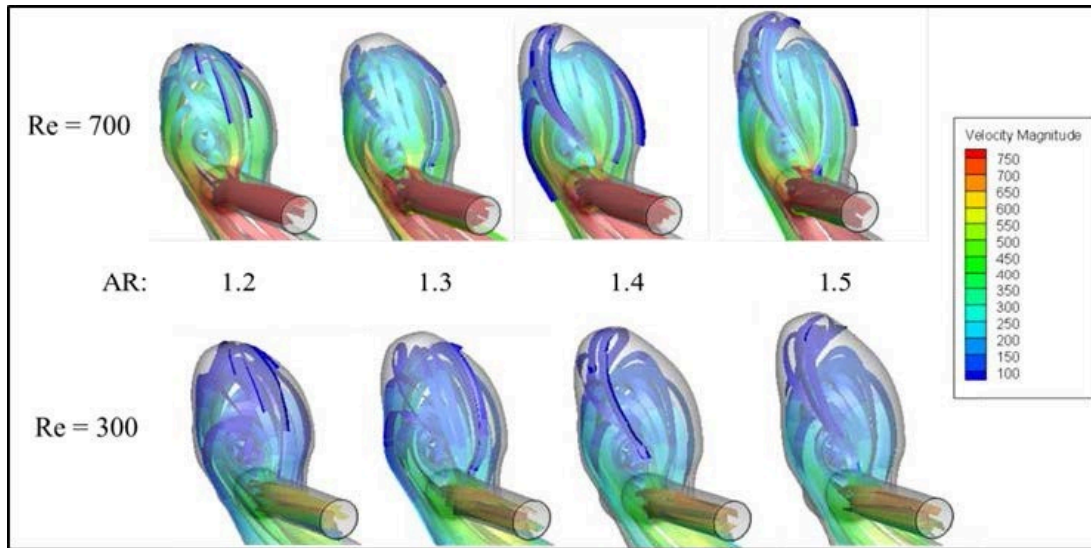
Figure 4.2. AR study re-conducted at different Reynolds numbers

The data in Figure 4.2 suggests that flow type prediction given by the critical AR equation is not affected by the parent artery Re. The transition region occurred between ARs of 1.3 and 1.4 for both Re sets, as well as with the original AR study. Because the Re study encompassed Reynolds numbers which covered the majority of the Re range for blood flow in the circle of Willis, the Re study suggests that critical AR equation is valid for most cases whose flow rates are physiological.

4.3   CONCLUSION

The critical AR equation has been developed for predicting the flow structure in a basilar artery bifurcation aneurysm; such information could be helpful to clinicians for assessing the health of the aneurysm by providing a description of the hemodynamics present. However, information presented in Sections 3.3 - 3.6 alluded to the notion that simply knowing the flow type in an

aneurysm may not provide a complete description of the hemodynamics. For example, it was shown that some instances of Type I flows can possess regions of lower velocities than other instances of Type II flows. Furthermore, it was shown that the severity of low flow regions can vary among exclusively Type I or exclusively Type II flows in such a way that the severity of slow flow in some Type I flows can exceed the severity of those found in other Type II flows. Therefore, a more complete description of the hemodynamics present in the aneurysm is needed as opposed to simply knowing whether an intra-aneurysmal flow is Type I or Type II. To accomplish a better description of intra-aneurysmal hemodynamics, WSS was studied in the next study. Particularly, the manner in which flow type influences both the WSS magnitude and the size of the region(s) where detrimentally low WSS exists needed to be examined. The findings of the effect on WSS from flow type will be presented in the next section of this work.

5.0   FLOW STRUCTURE AND CORRELATIONS WITH ITS IMPACT ON WALL

SHEAR STRESS

5.1   INTRODUCTION

A theory which predicts the type of flow structure within a basilar bifurcation aneurysm using AR, BF, and SI has been developed. The theory, however, only serves as a means of predicting flow structure within a bifurcation aneurysm; it does not make any prediction as to the hemodynamic loading on the wall. Of course, the existence of a secondary vortex, which can be predicted by the theory, serves as an indication that unfavorable hemodynamic conditions are present within the aneurysm. The single parameter studies, however, suggested that, by itself, the existence of a secondary vortex may not serve as a sufficient indicator which suggests the absence of adverse WSS. Rather than responding to a global flow pattern however, endothelial cells respond to the localized hemodynamic loading on the wall as opposed to the global nature of a flow pattern, and it is the hemodynamic loading on the wall which the intra-aneurysmal flow imparts that is of ultimate clinical significance in this study. The solutions of the models produced in the single variable studies are therefore re-visited with the focus being primarily on WSS.

The WSS contours were obtained for all of the individual characteristic parameter study groups from which progressive WSS trends were observed. Then, calculations for both area and

percent area below a certain critical WSS were made. These calculations were used as a metric to assess the well-being of the wall, in that an aneurysm with a larger region of low WSS would be considered as having a greater risk of rupture than an aneurysm with a smaller region of low WSS. Attention was paid to the flow type present for each case for which the WSS-area calculations were made. This method was used to determine extent to which the number of vortices present in an aneurysm could be used to indicate the hemodynamic conditions of the aneurysm, particularly near the dome region.

In healthy arteries, a normal range of WSS is considered to between 1 and 7 Pa [4]. A value of 0.4 Pa is reported to begin the range of unhealthy sub-physiological WSS [4]. A value motivated by this work of 0.1 Pa was used in the present study. The cutoff value must be intended as a more qualitative rather than quantitative marker. In a clinical setting, flow rates vary from patient to patient; the flow rate will vary even within each patient during levels of different physical activity. Often, patient-specific velocity information is unavailable. Furthermore, flow rates among the arteries of the cerebrovascular network also differ; therefore the application of the WSS study results to any general case must be made in a qualitative manner. Therefore, the cutoff WSS value will be used only as a reference point to demonstrate the WSS trends with respect to flow type and the parameters.

5.2   WALL SHEAR STRESS AND ASPECT RATIO

The WSS contours for the critical AR study show that as AR increases, so too does the region of low WSS in the dome region (Figure 5.1). The quantification of the low WSS area demonstrates

a monotonic trend between AR and low WSS as the second vortex grows in size with the enlarging dome region (Figure 5.2). Therefore, when considering the effects of AR alone, the data suggests that a Type II flow pattern is a necessary and sufficient condition for the existence of regions of low WSS. The magnitude of AR determines the size of the region of low WSS harbored by the secondary vortex. This is caused by the primary vortex neither enlarging nor slowing as the aneurysm volume is enlarged (see Figure 3.5), while the volumetric inflow remains nearly constant (see Figure 3.6). The result of these two factors must necessarily be that the region of the slow-moving secondary vortex must expand and thus the area of detrimentally low WSS must also expand.
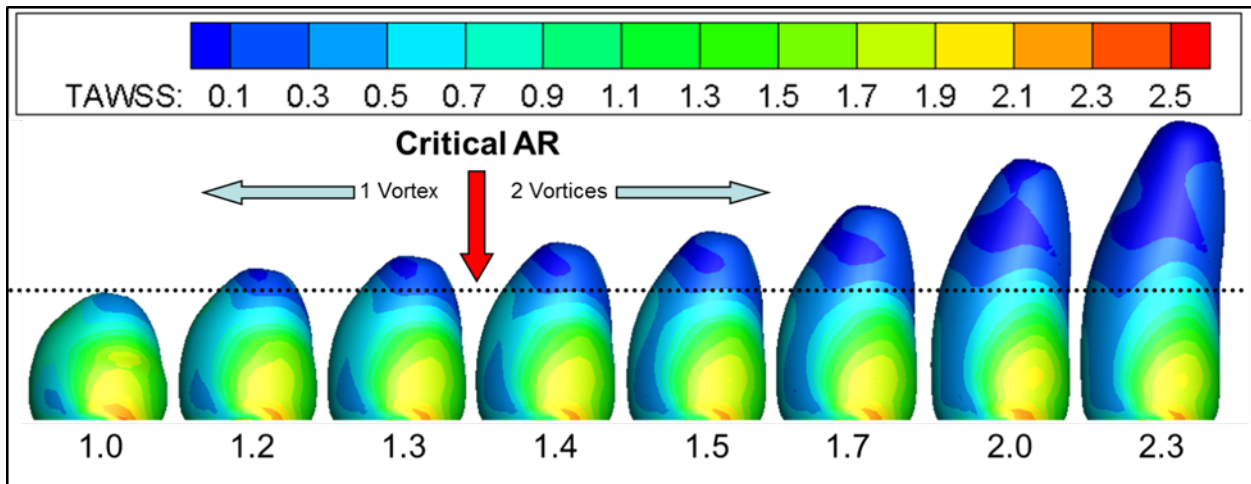
Figure 5.1. WSS distribution with varying AR
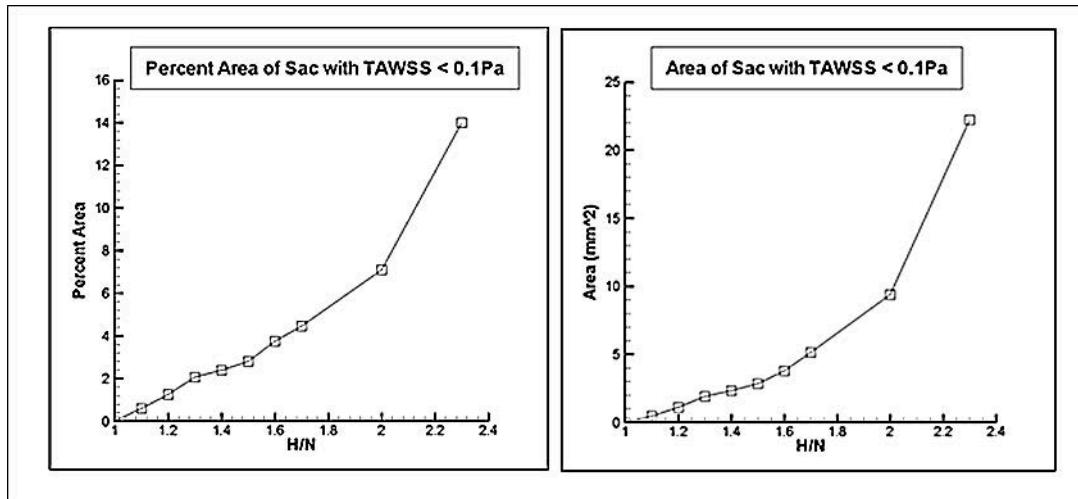
Figure 5.2. Percent area and area of WSS below 0.1 Pa with varying AR

5.3 WALL SHEAR STRESS AND BOTTLE-NECK FACTOR

Unlike what was found in the AR WSS study, the BF WSS study revealed a non-monotonic trend in low WSS with respect to increasing BF. Areas of pronounced low WSS are seen in models having both Type I and Type II flow patterns. This is possible due to two simultaneously competing factors. As BF increases, the primary vortex is able to occupy more of the aneurysm until it consumes the volume where the secondary vortex had once been. However, as BF increases, the volume of the aneurysm must necessarily increase to accommodate the larger cross-sectional diameters. It was shown previously that as the aneurysmal volume increases, there is no increase in the aneurysmal in-flow compensating for the increase in volume. The area of low WSS therefore increases again as the aneurysmal volume continues to increase. The results demonstrate that the optimally low area of low WSS exists at a BF of approximately 1.5, where the two inversely acting effects exist in a combination optimal for minimizing the low

43

WSS area. While for this study the Type I flow pattern demonstrated the best hemodynamic conditions on the wall, the Type I flow pattern also proved to promote as poor of hemodynamic conditions as the Type II flow pattern with a higher BF. Therefore, when considering the effects of BF only, a Type II flow pattern is only a sufficient condition for the existence of regions of low WSS: there may also exist Type I flow patterns for aneurysms which yield as poor of hemodynamic conditions as a Type II pattern if the BF is larger than 1.5 (Fig 5.3, 5.4).
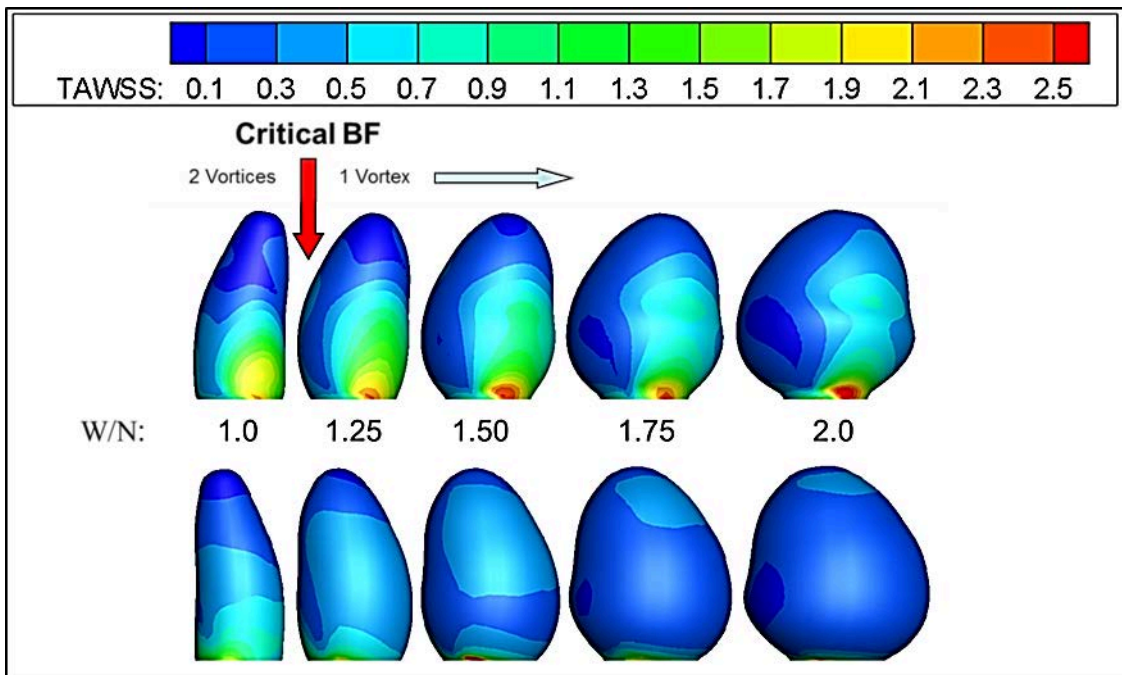
Figure 5.3. WSS distribution with varying BF
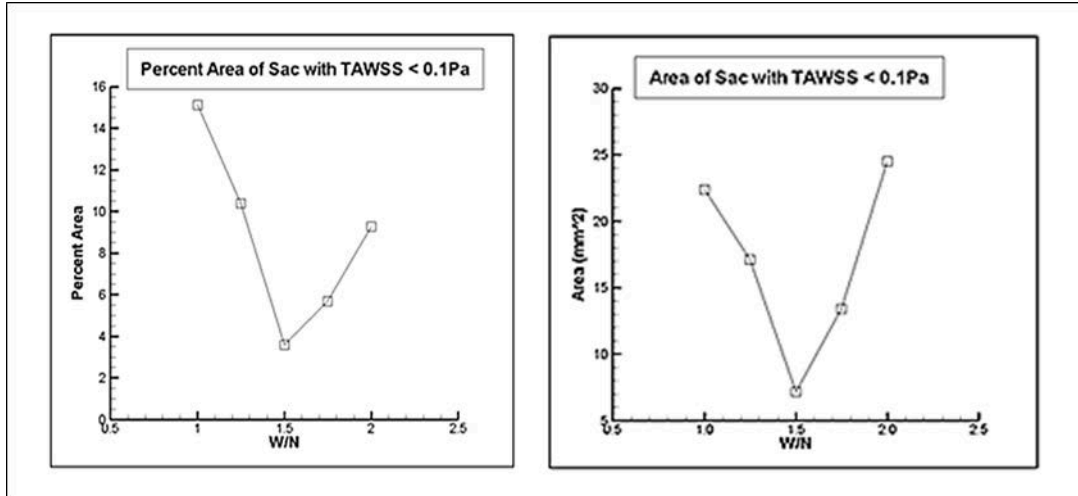
Figure 5.4. Percent area and area of WSS below 0.1 Pa with varying BF

5.4   WALL SHEAR STRESS AND SIZE INDEX

Like the trend found in the BF WSS study, the SI WSS study also revealed a non-monotonic trend in low WSS with respect to decreasing SI. Areas of markedly low WSS are seen in models having both Type I and Type II flow patterns. Similar to the BF study case, the non-monotonic WSS trend is possibly due to the two simultaneously competing factors of WSS increasing as the primary vortex is increasingly able to occupy more of the increasing aneurysm volume versus the lack of inflow compensation for the increase in aneurysmal volume in keeping WSS above a healthy level once the aneurysm's volume increases past a certain point. In the higher-valued SI case where the primary vortex was seen to exist below the aneurysm, a region of high WSS exists. This suggests that significant resistance to the flow entering is encountered due to the neck being smaller than the parent vessel diameter. As the neck enlarges, more inflow is met with less resistance as the WSS on the neck drops.

45

In Figure 5.5, it is seen that none of the cases shown contain WSS below 0.1 Pa despite the largest aneurysm having a neck diameter three times that of the parent artery diameter. This model demonstrates a case in which a relatively large aneurysm contains no levels of detrimentally low WSS, as opposed to the smallest model displayed in Figure 5.6. This notion is most probably due to the AR of the large aneurysm being close to 1.0 in conjunction with the flow type being a Type I flow. Furthermore, the BF is also close to 1.0; this eliminates extra volume in the aneurysm while the large ratio between the neck and parent artery diameter eliminates the need for a higher BF to keep the flow within the Type I regime. These notions can offer insight as to why some large aneurysms do not rupture: that despite them being large, their values of AR, BF, and SI are all defined with respect to each other in such a way that a flow exists in the whole of the aneurysm that is sufficient to avoid imparting sub-physiological and detrimental WSS on the aneurysm. A general example of such a case could be a large spherically shaped aneurysm having a small aspect ratio. The WSS behaves similarly with varying SI in aneurysms with higher aspect ratio; the only difference being that areas of low WSS primarily near the dome are more pronounced due to the higher aspect ratio (as shown in Figure 5.6).
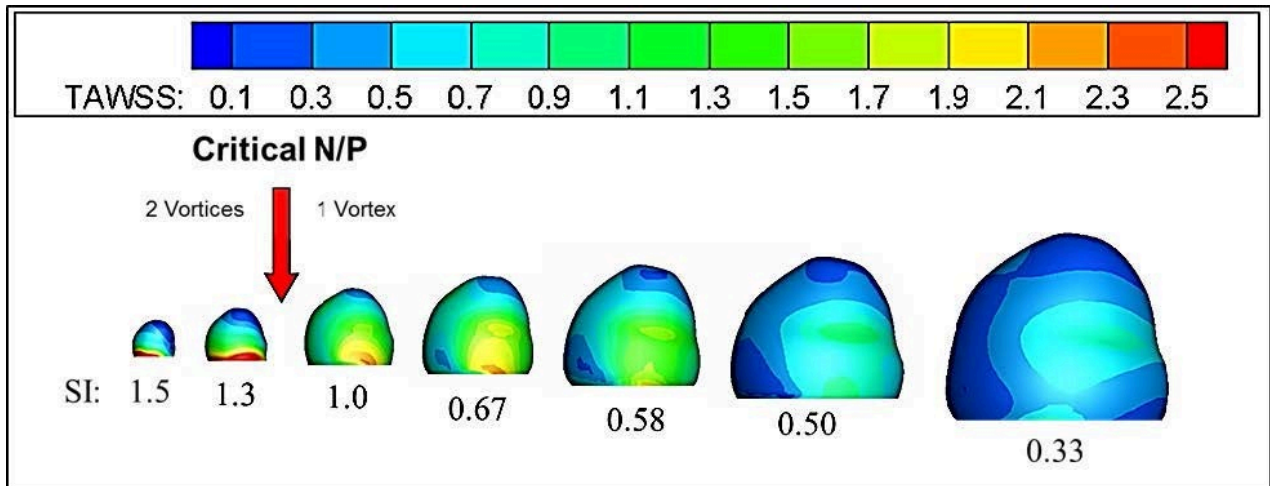
Figure 5.5. WSS distribution with varying SI
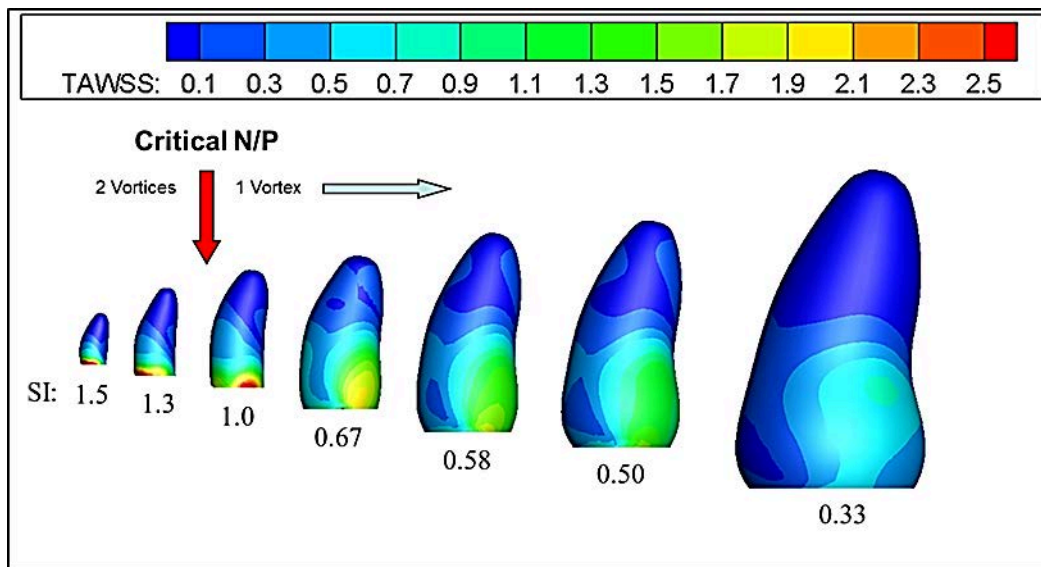
Figure 5.6. WSS distribution with varying SI for exclusively Type II flows
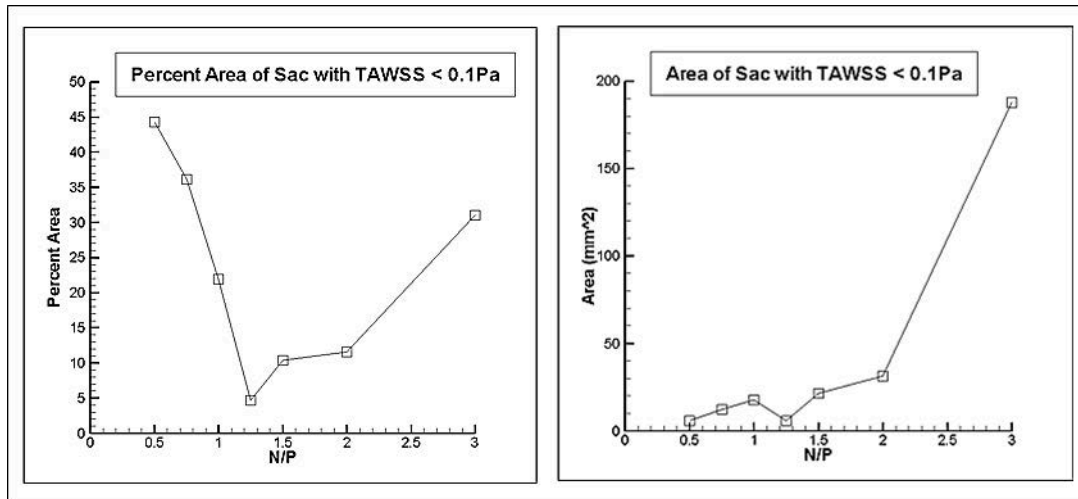
Figure 5.7. Percent area and area of WSS below 0.1 Pa with varying SI for exclusively Type II flows

5.5   WALL SHEAR STRESS AND CONICITY PARAMETER

It was shown in Section 3.6 that CP has no effect on determining whether the flow type within an aneurysm is Type I or Type II. However, it was noted that important qualitative features of the flow pattern are determined by CP: the degree to which the circulation occupies the aneurysm (if the flow is Type I) and the size of the secondary vortex (if the flow is Type II). In Figure 5.8, the WSS trends are shown for the Type II flow study. It can be clearly seen that, despite CP having no effect on determining flow type, the degree to which the level of low WSS varies as significantly in the CP study as it does in the other studies which directly impact the flow type. The effect on WSS for Type I flows is not as profound. A CP of 0.75 versus a CP of 0.33 had the effect of eliminating the 4% of the aneurysm area with WSS under 0.1 Pa in the 0.33 CP model. This evidence suggests that for Type I flows, a higher CP has the effect of allowing more flow to reach the dome. Therefore, the effect CP has on WSS depends on whether the flow is Type I or

48

Type II. For Type I flows, the effect of a higher CP is somewhat desirable; for Type II, the effect, as shown in Figure 5.9, can be quite detrimental.
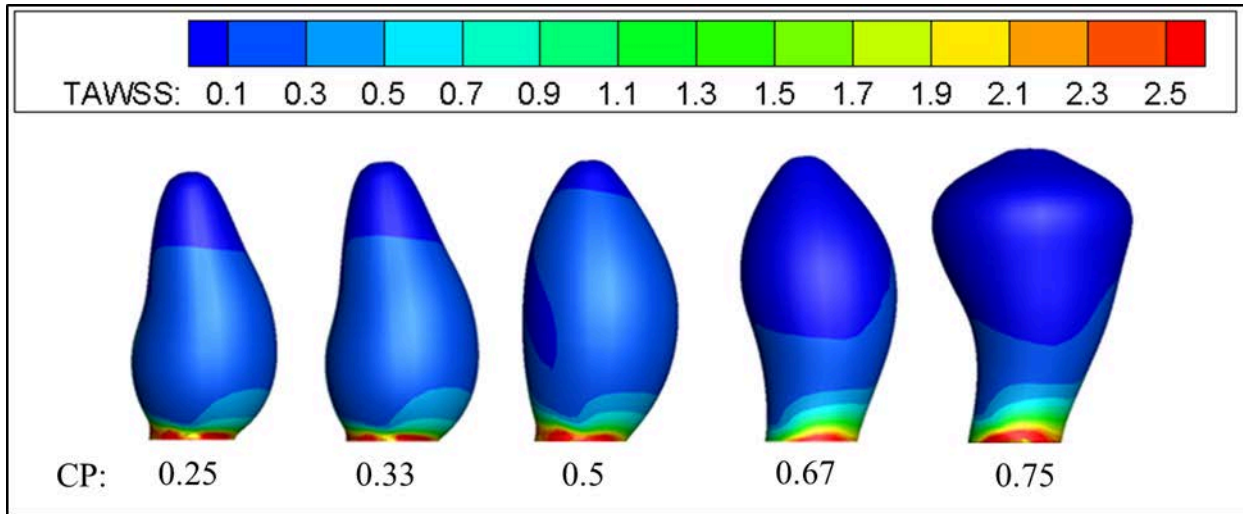
Figure 5.8. WSS distribution with varying CP
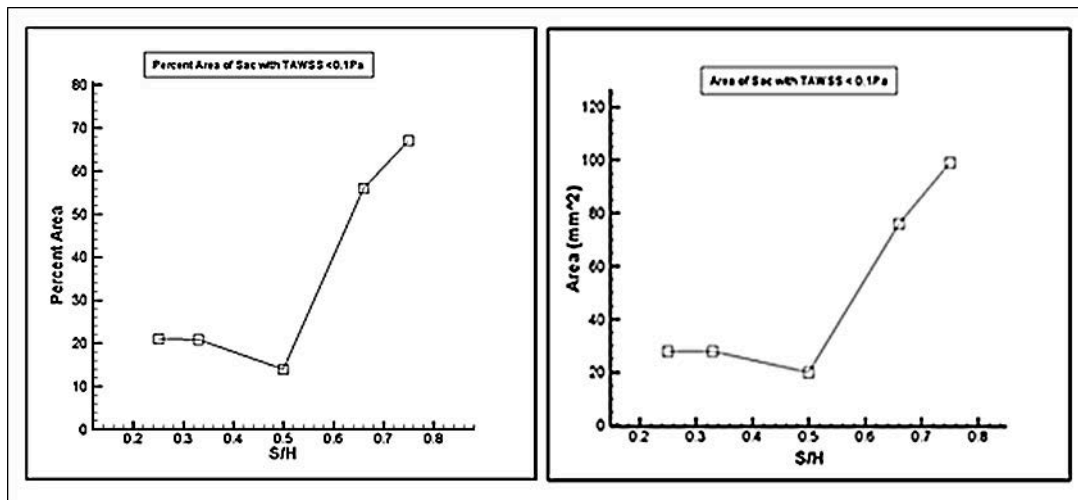
Figure 5.9. Percent area and area of WSS below 0.1 Pa with varying CP for exclusively Type II flows

5.6   DISCUSSION

The WSS data strongly suggests that the existence of a Type II flow within an aneurysm is a sufficient condition to produce regions of low WSS within an aneurysm. However, the WSS data has also demonstrated that the existence of a Type II flow is not a necessary condition for the existence of low WSS regions within the aneurysm, as the data shows that regions of low WSS can exist in aneurysms with Type I flow. The data suggests that the existence of low WSS regions in Type I flows is due to the fact that geometric conditions which inhibit Type II flow require an increase in the general size of the aneurysm. The increase in aneurysmal size however is not met with a significant increase in blood flow to the aneurysm (in some cases, the intra-aneurysmal flow rate was shown to decrease as the aneurysm became larger). Therefore, despite there being only one vortex present, low WSS is present. In terms of promoting low or higher WSS, the functions of the characteristic parameters and flow types are summarized in Table 5.1

Table 5.1. Summary of geometric parameters' effects on WSS

Parameter	Can an increase promote higher WSS?	Can an increase promote low WSS?
AR	No	Yes
BF	Yes	Yes
SI	Yes	Yes
CP, Type I	Yes	No
CP, Type II	No (Slight increase for 0.0 < CP < 0.5)	Yes
Flow Type	Promoter of Higher WSS?	Promoter of Low WSS?
Type I Flow	Yes	Yes
Type II Flow	No	Yes

From Table 5.1, it is sufficient to propose that unhealthy conditions exist in a bifurcation aneurysm if Type II flow is present; the severity of the unhealthy conditions can be estimated primarily by AR and CP since their trends are monotonic for this flow type; however, BF and SI can also be employed for a more accurate estimate of the hemodynamics. Any increase in AR, CP, or both would only make the unhealthy conditions in a Type II flow worse (provided CP > 0.5, if CP < 0.5, increasing it has a small effect on increasing WSS). However, the effect on hemodynamic conditions being more desirable or more detrimental from an increase in BF or SI would be dependent on the initial value of BF or SI due to the non-monotonicity of the BF and SI trends.

Because of the non-monotonicity of the BF and SI trends, determining the extent to which low WSS is present in aneurysms with Type I flows (if present at all) is not nearly as straightforward. In this situation, the volume of the aneurysm would be the best indication of the state of hemodynamic conditions. If the aneurysm volume is too large (i.e., SI is too small or BF is too large), then the intra-aneurysmal blood flow is not adequate to produce healthy levels of WSS. However, if SI is too large or BF is too small, then the flow would exist as a Type II flow. Finally, the extent to which the AR is below the critical AR for aneurysms with Type I flows can serve as a valuable indicator to the presence of low WSS within a large aneurysm with Type I flow. Therefore, the following can be proposed. If the BF, SI, or both trend away from their WSS optimal values such that the aneurysmal volume is increased, the flow will remain Type I, however the hemodynamic conditions will worsen despite the Type I flow. If the BF, SI, or both trend away from their WSS optimal values such that the aneurysmal volume is decreased, then the flow becomes ever closer to transitioning to a Type II flow, which is a sufficient condition for poor hemodynamics. A healthy Type I flow is therefore proposed to exist in aneurysms

51

where BF and SI are between their optimal values and their values which would cause a Type II flow to exist. From the data produced in the study, it seems that a healthy WSS optimal SI value is approximately 0.8, and a corresponding BF value is approximately 1.5. However, the combine effects of multiple characteristic parameters on WSS have not yet been studied; the optimal SI and BF may vary for other cases. Therefore, with the amount of data available, the obtained optimal values should be used only as approximate guidelines for determining WSS conditions for Type I flows. A summary of the proposed criterion for determining whether an aneurysm is at significant risk of rupture based on containing regions of low WSS is presented in Figure 5.10.
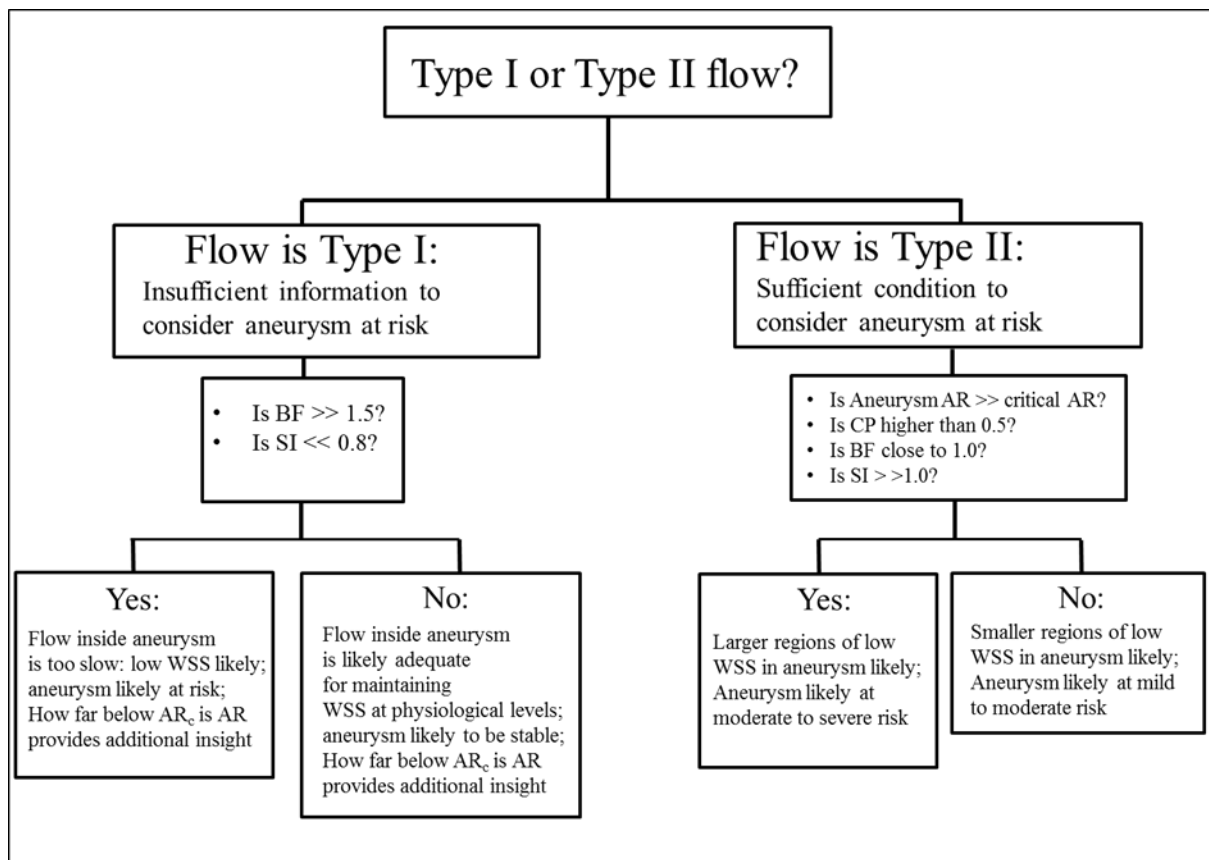
Figure 5.10. Flow chart of the process of approximating hemodynamic conditions in a bifurcation aneurysm using clinically available geometry

Aside from serving as a guide to physicians as to the state of the hemodynamic loading on the aneurysm wall at one time instant, the theory developed in this work can serve as a means of describing the positivity or negativity of a change in aneurysmal geometry. Aneurysms grow and remodel over time [17]. With respect to promoting or deterring adverse WSS, the theory established in this work can be used to judge whether a particular change in the aneurysmal geometry is a positive change or a detrimental one. As an example, an aneurysm having a BF equaled to 1.0 at one time instant with a Type II flow pattern will be considered. The aneurysm in the example will require a BF of 1.3 to transition from a Type II flow to a Type I flow. If at future time instant the BF is found to enlarge to 1.4 such that a Type I flow results from the change, then the change in BF could be thought of as the aneurysm remodeling to promote healthier conditions. However, if the BF were to have instead enlarged to 3.0, then the change could be thought of as detrimental, as the remodeling would bring about worse hemodynamic conditions. In this manner, the developed theory in this work can be used to determine whether aneurysmal growth is favorable or unfavorable, and in particular, exactly what geometric aspect of the new growth is responsible for promoting the new conditions.

While the parametric study has produced a sketched outline which describes the nature of intra-aneurysmal flow dynamics that in particular serves as a tool able relate the combination of aneurysmal size and shape to shear stress imparted on the wall, it cannot be considered a complete guide to determining whether an aneurysm will rupture. While slow-moving blood flow and its resulting effects within an aneurysm and has been hypothesized to be a mechanism responsible for aneurysmal growth and rupture, it is not the only factor believed to influence this matter [1,17]. The biology of how the IA wall reacts to low WSS, as well as processes within the aneurysm wall unrelated to WSS venture beyond the scope of this study and are not

considered here. Just as AR on its own cannot completely describe the flow conditions, the WSS magnitude in aneurysms on its own cannot completely describe the state of the aneurysmal wall [1,17]. The work presented here is therefore intended only to provide a means of determining one particular known risk factor (low aneurysmal WSS) to be weighed among other factors in ultimately deciding whether or not an aneurysm is likely to rupture.

5.7   CONCLUSION

It has been shown that the existence of a Type II flow in a bifurcation aneurysm is only a sufficient condition for the presence of low WSS. Aspect Ratio and in most cases, Conicity Parameter, can be used to determine the severity of the low WSS region brought about by Type II flows. It is possible however for an aneurysm to have low WSS with a Type I flow. For this instance, no definitive quantitative criterion has been defined for the existence of low WSS. However, general qualitative trends have been established as to what features of the aneurysm are responsible for promoting and deterring regions of low WSS, and guidelines based off the data from the study have been proposed.

The ability to predict a Type II flow is a valuable asset because a Type II flow is a sufficient condition to alert a clinician that regions of low WSS exist within an aneurysm. The severity of the low WSS region can be judged by knowing how far above the critical AR is the AR of the aneurysm of interest, and by knowing whether the CP is high (specifically, greater than 0.5). By using the equation developed to predict AR, a clinician would be able to determine if the sufficient condition of Type II flow is present in a patient's aneurysm. However, the theory

developed to this point upon which the critical AR equation has been derived only from the numerous parametric models which all stem from one original reference model of an aneurysm located at the tip of a basilar bifurcation. Considering the analysis presented thus far, nothing can be stated regarding the theory's applicability to different aneurysms located on different parent geometries. Furthermore, the information presented cannot determine whether idealizations made in the parametric analysis would significantly impact the critical AR equation's effectiveness at predicting the flow type in a clinical setting. For example, no study was done to determine whether elliptic cross sections have a different effect on the flow structure versus the effect from circular cross sections. A clinical validation study was therefore required to assess whether the analysis thus far presented is applicable to a clinical setting and is presented in the next section.

6.0   VALIDATION OF DEVELOPED CORRELATIONS USING CLINICAL

MODELS

6.1   INTRODUCTION

An equation which predicts intra-aneurysmal flow type has been developed from a parametric study of an aneurysm located on the tip of the basilar artery bifurcation. Before the theory can be considered of value to a clinical setting, the applicability of the theory to a clinical setting must first be assessed. Most importantly, the critical AR equation developed from the study of parametric bifurcation aneurysms must be able to predict the flow type in real bifurcation aneurysms. Provided the critical AR equation can be applied to real aneurysms, it is furthermore desired that the theory need not be restricted to only predicting the flow type in basilar artery bifurcation aneurysms, but rather that the theory be applicable in general to any bifurcation aneurysm. To assess whether the two outlined conditions are plausible, a validation study consisting of 27 bifurcation aneurysms was conducted. In the validation study, numerical models of each of the 27 clinical geometries were produced; the velocity fields of which were approximated using the Adina finite element-based solver, and the flow type for each case was obtained. The flow type obtained from the numerical solutions of the models was then compared

56

with the flow type predicted from the critical AR equation for each case. From this study, an assessment of the applicability of the critical AR equation to a clinical setting was produced.

In the parametric study, multiple idealizations were made, and potentially important characteristic geometric features were neglected. Perhaps one of the most potentially influential idealizations in the parametric study was the usage of circular cross-sectional geometry in the parametric models. Real aneurysms, as well as vasculature in general, are not confined to possessing circular cross-sectional geometry. This notion could be potentially problematic for the theory's success in predicting critical AR by two means. One is that the effects on flow structure from elliptic geometry have not been evaluated in the parametric study, and therefore, these effects are unknown and have not been factored into the critical AR equation. Second, it is not clear as to what value of, for example, neck diameter, should be used for the prediction of flow type in the case of an elliptic neck cross-section, as no parametric study had been performed to resolve this issue. By this notion, even if elliptic versus circular cross-sectional geometry were to insignificantly affect flow structure, simply selecting un-representative values for use in the critical AR equation may cause the theory to yield incorrect predictions. Other previously-made potentially idealizations, both known and unknown could affect the theory's effectiveness as well. Moreover, the case selected as the original reference model for the parametric study was selected in part due to its general geometric simplicity. The aneurysm centerline was relatively straight with no significant bends or curvature. The surface shape was unilobular as opposed to having a high undulation with many inflection points and multiple lobes; the surface in general was smooth with little distinctive features. The parametric reconstruction of the original reference model furthermore smoothed the already-smooth surface. With respect to the parent geometry, the out-of-plane angle made between the aneurysm and parent vasculature was nearly

zero, which indicates that the aneurysm centerline is oriented parallel the direction of incoming flow: this is not the case for some aneurysms. It was furthermore assumed that the aneurysm was situated directly on the parent geometry: that the volume swept along the centerline in the neck region was minimal, such that there was no elongation of the neck region. An elongated neck region would not only introduce complications in defining the characteristic parameters, but would also introduce further resistance of blood flow into the aneurysm, particularly in the case of a high SI or a low BF. Lastly, no modifications were made to the parent vasculature during the course of the parametric study in its entirety; therefore, any sensitivity of the flow structure to variations in parent geometry had not been considered.

A clinical case needed to meet specific requirements to qualify for inclusion in the study. Because the original theory was developed for bifurcation aneurysms, the validation study must be restricted to include bifurcation aneurysms only; sidewall aneurysms were therefore excluded. In short, the flow entering a bifurcation aneurysm enters mainly normal to the neck plane; whereas flow entering a sidewall aneurysm enters in a manner more tangent to the neck plane. Thus, different flow dynamics incongruent with each other should be expected amongst these two types of aneurysms, and sidewall aneurysms must therefore be excluded from the theory. To qualify as a bifurcation aneurysm, the centerline of the parent vessel must extend through any point in the neck plane of the aneurysm. Furthermore, the parent vessel must terminate into two daughter vessels; the aneurysm must be located on this termination. In a more abstract sense, the aneurysm neck must be located where flow from the parent vessel would have otherwise impinged had the aneurysm not been present. No further restrictions were placed on cases for inclusion in the validation study.

The 27 clinical cases were selected by their availability, and that they met the previously defined requirements for inclusion in the study. The solutions to their flow fields were approximated using the Adina finite element solver as with the parametric study, using the same general modeling assumptions and mesh grid criteria. All models used the same waveform boundary condition, as the patient specific data was not available for any of the models. For cares in which more than two outlets in the model were present (as opposed to the one inlet and two daughter branch outlets in the parametric study models), the modified traction boundary condition was applied to one outlet (regardless of the number of outlets); a prescribed velocity vector on each of the remaining outlets completed the boundary conditions on the outlets. Like with the parametric study models, the flow split was imposed such that the wall shear stress at each outlet was equal. The prescribed velocities at the inlets were approximated based on matching the systolic Reynolds number of each clinical case to that of the systolic Reynolds number in the models in parametric study. For the theory to prove to be robust enough to implement in a clinical setting, variation amongst patient specific information must be negligible. The usage of general boundary information is therefore considered to be appropriate.

Because of the non-ideal nature of the clinical models, a procedure to define H, W, P, N, and S for the validation study was needed. The aneurysm height, even in a non-ideal situation, is still defined by the linear distance from the center of the neck plane to the center of the dome, so H retained its parametric study definition. Due to non-uniform cross sections in clinical models, W, P, and N have no unique way of being defined as they had in the parametric study which implemented uniform cross-sections. To represent the full range of possible cross-sections, the maximum and minimum definable values of W, P, and N were measured. Two values of S were then obtained based off the distance between the neck cross-section and each one of the planes

where a W was defined. The final set of dimensional parameters included one H, and two Ws, Ps, Ns, and Ss, from which two ARs, four BFs, four SIs, and two CPs were defined. Because no parametric study was performed to justify a method of weighting the maximum and minimum cross sections, the simple average between the maximum and minimum values of the parameters was evaluated to produce the average valued characteristic parameters (H∕N)avg, (W∕N)avg, (P∕N)avg, and (S∕H)avg . The critical AR equation was then modified to be

$$AR_{critical} = 2.5 \ (\frac{W}{N})_{avg} - 0.92 \ln(\frac{P}{N})_{avg} - 1.5$$

The $(H/N)_{avg}$ was used as the means of comparison with the calculated AR from the averaged critical AR equation to determine whether or not the AR of each case exceeded the critical AR.

6.2   CLINICAL MODELS

Among the 27 clinical models, 16 cases exhibited Type I flow, 10 cases exhibited Type II flow, and one case exhibited both types of flow in what appeared as two separated aneurysms fused together. Thirteen of the 27 aneurysms met within reason all assumptions which were made for the parametric study; all but two of these aneurysms had Type I flow. The rest of the aneurysms contained at least one significant aspect not considered in the parametric study; the most common of which was cross-sectional ellipticity, which was significant in six of the cases. Significant cross-sectional ellipticity was defined by the model having at least one non-dimensional characteristic parameter for which the difference in maximum and minimum

dimensional parameter values which comprise the non-dimensional parameter was greater than

25% of the average value of the dimensional parameters. Mathematically, this relationship is

given by $\frac{A_{max}-A_{min}}{A_{avg}} \geq 0.25$, where A is any general dimensional parameter relevant to the study

contained within the aneurysm. With respect to other previously-excluded aspects, four of the

cases had a bleb on the aneurysm dome, and one of the cases had a bleb on the side wall of the

aneurysm. Three of the cases had aneurysms oriented nearly 90 degrees off the parent vessel

centerline, three cases had significant undulation (e.g. they were not unilobular), and one case

had an elongated neck region. Many cases which possessed more than one excluded criterion

were of Type II flow. Figure 6.1 provides a visual demonstration of idealizations proven to have

a significant impact on the study. The range of parameters tested in this validation study is

tabulated in Table 6.1 and Table 6.2 summarizes the flow structures in the set.
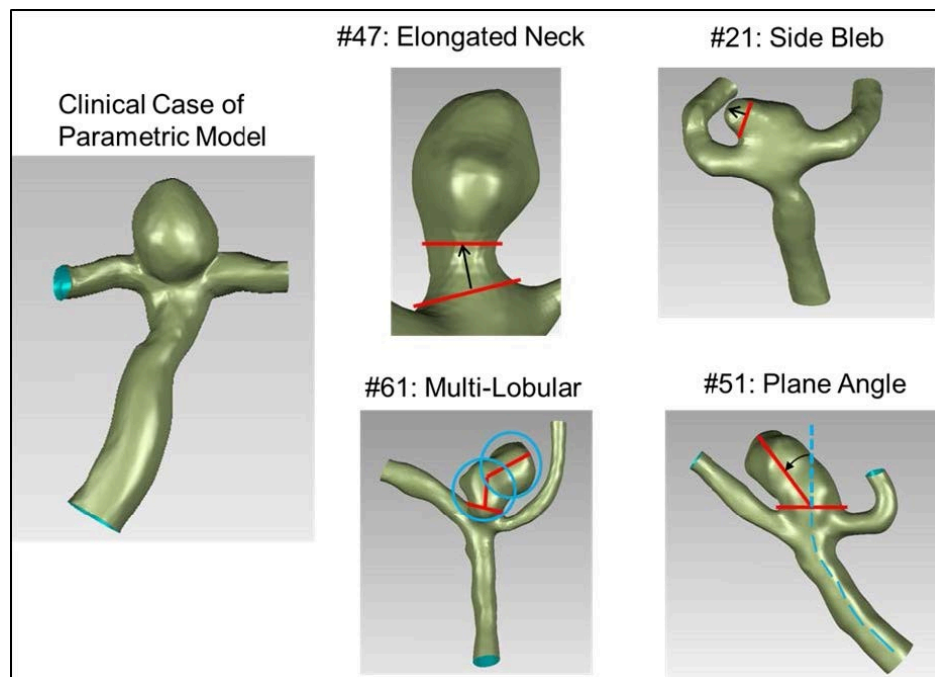
Figure 6.1. Illustration of violations of some important idealizations assumed in the parametric study

Table 6.1. Range of parameters for validation study models

Range of Parameters in Validation Study				
	H/N	W/N	P/N	S/H
Min	0.6	1	0.32	0
Max	2.3	1.8	1.2	0.65
Average	1.4	1.3	0.74	0.31

Table 6.2. Flow structure distribution among the 27 clinical cases

Distribution of Flow Structure in Set		
Type I Flow	Type II Flow	Non-Applicable Models
59%	37%	4%

6.3   EVALUATION OF CRITICAL ASPECT RATIO EQUATION'S ACCURACY

FOR CLINICAL CASES

Using the averaged characteristic parameters, the critical AR equation correctly predicted the flow type in 24 of the 26 cases for which it was possible to define the characteristic parameters. The equation would have failed to predict the flow pattern in three of the 24 correctly predicted cases had the extreme (maximum or minimum) values been used as opposed to the averaged values in the definition of the parameters. For another two cases, the equation failed to predict the flow type regardless of whether maximum, minimum, or averaged values were used in the equation. One of the failed cases had a significantly elongated neck region, which is thought to

be the cause of failure. The equation predicted that the flow should be Type I. However, the elongated neck caused greater flow restriction than there would have been had the neck region been shorter. The result was that the primary vortex occupied the bifurcation region in the parent artery, while the slower secondary vortex completely occupied the aneurysm. The elongated neck presumably amplified the effect seen in the SI study in Section 3, when the ratio of the parent artery to the neck diameter became greater than unity. The equation also failed to predict a Type II flow in an aneurysm which had a bleb on the side wall. While four other aneurysms contained blebs near to the size of the side bleb in the failed case, the other four cases contained blebs on their domes (dome blebs) as opposed to on the side wall (side blebs). Dome blebs did not affect the flow type. The side bleb, however, contained its own vortex, possibly due to the fact that the opening to a side bleb is tangent to the flow entering the aneurysm as opposed to the dome blebs being oriented more normal to the flow entering the aneurysm. The overall effectiveness of the critical AR equation is summarized in Table 6.3 and a summary of the excluded geometric aspects in the parametric study are included in Table 6.4. The systolic streamlines of both cases for which the critical AR equation completely failed are shown in Fig 6.2.

Table 6.3. Effectiveness of the critical AR equation

Overall Effectiveness of Theory			
Correct: Avg or Extremes	Correct: Avg Only	Incorrect	Non-Applicable
78%	89%	7%	4%

Table 6.4. Tabulation of some geometric aspects not considered in the original parametric study and how they impact the critical aspect ratio prediction

Geometric Aspects Excluded in Original Theory and Effect on Flow Type Prediction						
	Elliptic CrsSctn	Top Bleb	High Undulation	Sac Orientation	Side Bleb	Elongated Neck
Number:	6	4	3	3	1	1
% of Cases	22%	19%	11%	11%	4%	4%
Error with Max/Min?	3	0	0	1 (also elltp. CrsSctn)	0	0
% of Cases	11%	0%	0%	4%	0%	0%
Error with Max/Min/Avg?	0	0	0	0	1	1
% of Cases	0%	0%	0%	0%	4%	4%
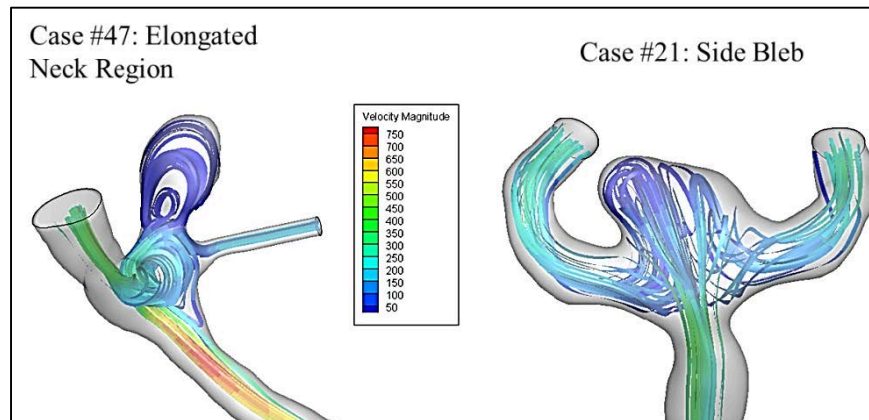
Figure 6.2. Systolic streamlines of cases for which critical AR equation failed to predict flow type

To further assess the critical AR equation's predictive accuracy, the validation cases containing Type II flow structures were further analyzed to evaluate whether the critical AR equation accurately predicted the severity of the Type II flow structure, particularly with borderline cases. The significance of the evaluation is the following. If the AR of an example

case is merely 0.1 greater than the calculated critical AR, then by the data shown in Figure 3.5 of Section, one would expect that the Type II flow structure should borderline Type II, i.e., the secondary vortex should be small with respect to the primary vortex. If however the actual flow structure of the same case contains a large secondary vortex (given that S/H is small), then the possibility exists that the critical AR equation significantly over-predicted the critical AR by enough to neglect important information regarding the severity of the case, but not by enough to incorrectly predict the flow type. Furthermore, the possibility may arise that had the AR in the example been 0.2 less, the flow type could have still been Type II, yet the critical AR equation would have predicted a Type I flow pattern. Such an example suggests that without further evaluation, false confidence could be placed in the critical AR equation's abilities to otherwise perfectly predict the flow-type for any bifurcation aneurysm which does not contain side blebs or elongated neck regions. Furthermore, the unstudied effects of parameters such as ellipticity or plane-angle which heretofore have not shown to be confounding could in actuality impact the flow structure while remaining undetected unless further analysis is conducted.

Appendix A contains a tabulation of all four non-dimensional parameters for each validation case, their predicted and actual number of vortices, and the amount by which the AR of each case was under or over the predicted critical AR. Appendix B tabulates the violations of the geometric assumptions per case implemented in the parametric study. Using the information in Appendix A in conjunction with analyzing the systolic streamlines of each case, it is possible to assess whether the difference in critical AR from AR for each case corresponds to the extent to which the Type II flow pattern is predicted. Furthermore, using the information in Appendix B in conjunction with the systolic streamlines of each case provides a means of identifying other

parameters which were not studied in the parametric study which could affect critical AR. The results of the analysis of each predicted Type II case are summarized in Table 6.5.

Table 6.5. Assessment ability to predict the extent of the Type II flow pattern

Assessment of Type II Predictions		
Case	Accurate Type II Prediction?	Geometric Assumptions Violated
87	yes: Second vortex scales with AR-ARc	None
54	yes: Second vortex scales with AR-ARc	CrsSctn Ellipticity
15	yes: Large SI; primary vortex in bifurcation	CrsSctn Ellipticity
5	yes: Second vortex scales with AR-ARc	None
61	no: Large second vortex; AR-ARc = 0.04	Multi-Lobular, High Curvature in Centerline
51	no: Large second vortex; AR-ARc = 0.01	Multi-Lobular, Plane Angle
7	no: Large second vortex; AR-ARc = 0.06	Plane Angle, Top Bleb
6	no: Large second vortex; AR-ARc = 0.17	Plane Angle

Figure 6.3 compares the systolic streamlines between Cases 87 and 61: a case which holds true to the geometric assumptions in the parametric study and a case which violates two geometric assumptions from the parametric study. It is readily seen that the ratio between the sizes of the two vortices of Case 87 is consistent with that predicted by the AR study in Chapter 3; however this does not hold for Case 61, where the sizes of the two vortices are nearly equal despite the difference of 0.04 between AR and critical AR.
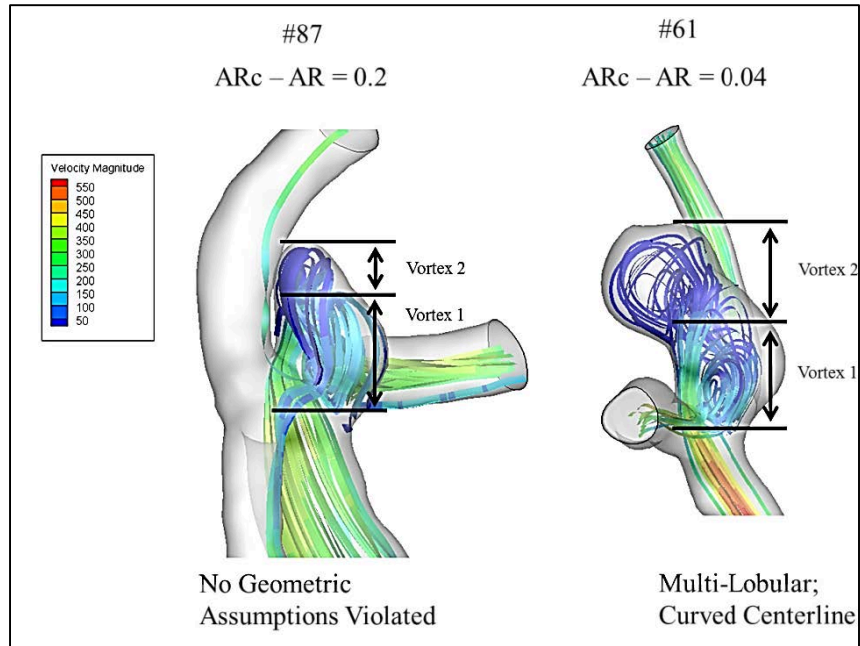
Figure 6.3. Systolic streamlines in cases which represent an accurate vs. an inaccurate prediction of the extent of the Type II flow

While the critical AR equation was 100% accurate for the Type II cases with no side blebs or elongated neck regions, the data in Table 6.5 and Figure 6.3 both suggest that the possibility for flow type error exist if more cases were to have been included; particularly cases with multi-lobular aneurysms (as demonstrated in Fig 6.3), or with aneurysms whose neck planes are not oriented normal to the parent vessel centerline. However, the effects of these attributes were not significant enough to cause an incorrect flow prediction as with cases 21 and 47, where the critical AR was over-predicted by 0.47 and 1.01 respectively. Regardless, the data presented in Table 6.5 and Figure 6.3 suggest that cases with borderline ARs should be considered as being well in excess of the critical AR if they contain a multi-lobular structure or a neck-plane angle effect.

6.4 EVALUATION OF CRITICAL ASPECT RATIO EQUATION'S SENSITIVITY TO ERROR IN MEASUREMENT

While the critical AR equation was able to successfully predict the flow structure in 24 of 26 (92%) of the applicable cases, the accuracy of the equation could be potentially limited by the process of obtaining the inputs to the equation. Obtaining improper values of H, N, W, and P is a strong potential source of error. Further error could be introduced by failing to obtain the properly averaged parameters. The sensitivity of the critical AR equation to error in obtaining the proper values of H, W, P, and N was evaluated for two scenarios: one in which the control dimensional and non-dimensional parameters were equal to unity, and the other in which the averaged values of AR, BF, and SI obtained in the study were used as the control values. In both single-variant error analyses, each parameter was varied by plus and minus 25% of the control value. For the scenario in which all control parameters are set to unity, the variation by ±25% corresponds to a spread which is half the average of 1.00. In the second scenario, the lowest spread among any parameter is ±36%. This analysis therefore provides a conservative estimate in potential error, as the largest spread found between any parameter in the clinical data set was 30% of the average. The error in critical AR prediction was then tabulated for each case, and the success or failure of the equation to predict the flow type for each case was noted. The results are summed in Tables 6.6 and 6.7.

68

Table 6.6. Sensitivity of critical AR equation to error in obtaining proper input parameters for case where

control parameters are unity

Critical AR Sensitivity to Dimensional Error: H = W = N = P						
	H/N	W/N	P/N	ARc	Diff % of ARc	Flow Type Err?
Control	1.00	1.00	1.00	0.97	-	-
-25% H	0.75	1.00	1.00	0.97	-	Yes
+25% H	1.25	1.00	1.00	0.97	-	No
-25% W	1.00	0.75	1.00	0.35	-65%	No
+25% W	1.00	1.25	1.00	1.60	+60%	Yes
-25% P	1.00	1.00	0.75	1.23	+27%	No
+25% P	1.00	1.00	1.25	0.76	-21%	Yes
-25% N	1.00	1.33	1.33	1.54	+59%	Yes
+25% N	1.00	0.80	0.80	0.68	-30%	No

Table 6.7. Sensitivity of critical AR equation to error in obtaining proper input parameters for case where

control parameters are study-average parameters

Critical AR Sensitivity to Error Considering Study-Average Parameters						
	H/N	W/N	P/N	ARc	Diff % of ARc	Flow Type Err?
Control	1.39	1.25	0.74	1.87	-	-
-25% H	1.04	1.25	0.74	1.87	-	No
+25% H	1.74	1.25	0.74	1.87	-	No
-25% W	1.39	0.94	0.74	1.09	-56%	Yes
+25% W	1.39	1.56	0.74	2.65	56%	No
-25% P	1.39	1.25	0.56	2.14	19%	No
+25% P	1.39	1.25	0.93	1.67	-15%	No
-25% N	1.85	1.67	0.99	2.65	56%	No
+25% N	1.11	1.00	0.59	1.45	-30%	No

From the error analysis, it is evident that improper values of W possess the strongest potential for

error, followed by values of N and lastly P.

6.5   CONCLUSION

The critical aspect ratio equation developed in the parametric study has been shown to be able to successfully predict the flow type in 24 (~92%) out of the 26 applicable clinical cases. Two geometric conditions have been identified which confound the equation's predictive abilities, and together serve as a notion that not all geometric aspects can be accounted for in a practical manner, and that some geometric aspects will cause the equation to fail. The validation set suggests however that the percentage of cases containing confounding geometry is small. The validation study outcome demonstrates that this work has developed a potentially useful tool for clinicians to implement in treating patients with IAs. Foremost, the theory developed in this work has demonstrated its ability to identify the existence of a sufficient condition for the existence of detrimental levels of WSS in bifurcation aneurysms; the existence of which has been hypothesized to be a risk factor leading to the rupture of aneurysms. The existence and severity of the condition can be determined by four characteristic geometric features; all of which are readily obtainable from angiography. Furthermore, particular types of geometries which do not possess the sufficiently low WSS condition of having a Type II flow but are still at risk for harboring low WSS were identified from trends in WSS produced by the parametric modeling method, providing new insight to the conventional method of considering all single vortex aneurysms less at risk of rupturing over those having two vortices. In addition to providing information regarding risk of rupture, the data from the parametric study suggests an approximate set point configuration for bifurcation aneurysms which have progressed past the stages of initiation such that WSS conditions are optimal for promoting favorable conditions for the endothelium to thrive. A change over time in the aneurysmal geometry can therefore be categorized as being beneficial versus detrimental by applying the theory formed in this work.

Furthermore, a particular feature in a remodeled geometry can be singly identified as being responsible for a change in the hemodynamics present. Ultimately, this study has demonstrated that correlations between one geometric parameter and the risk of rupture cannot be reliable if hemodynamics does indeed significantly impact the health of the aneurysm wall, since one geometric parameter is insufficient to describe intra-aneurysm hemodynamics on a general level.

APPENDIX A

CLINICAL MODEL DATA FOR VALIATION STUDY

Validation Study Case Information								
ID#	P/N	H/N	W/N	S/H	ARc	n Predicted	n Actual	AR-ARc
47	1.24	1.88	1.85	0.41	2.9	1	2	-1.01
21	0.52	1.10	1.00	0.00	1.6	1	2	-0.47
61	0.83	2.38	1.48	0.65	2.3	2	2	0.04
51	0.78	1.63	1.17	0.38	1.6	2	2	0.01
7	0.51	1.66	1.00	0.00	1.6	2	2	0.06
54	0.95	1.80	1.20	0.29	1.5	2	2	0.28
15	1.70	1.23	1.19	0.41	1.0	2	2	0.26
6	0.65	1.55	1.00	0.59	1.4	2	2	0.17
98	0.32	1.50	1.38	0.57	3.0	1	1	-1.49
66	0.70	1.36	1.25	0.42	1.9	1	1	-0.56
32	0.76	1.40	1.71	0.79	3.0	1	1	-1.59
68	0.55	1.03	1.25	0.31	2.2	1	1	-1.13
4	0.85	1.62	1.35	0.41	2.0	1	1	-0.38
5	0.88	1.76	1.14	0.36	1.4	2	2	0.32
87	0.98	1.27	1.03	0.39	1.1	2	2	0.20
78	0.69	1.07	1.09	0.38	1.5	1	1	-0.47
49	0.81	1.96	1.77	0.55	3.1	1	1	-1.14
96	0.35	1.42	1.24	0.46	2.5	1	1	-1.11
20	0.63	1.09	1.26	0.48	2.1	1	1	-0.97
11	0.48	0.90	1.10	0.60	1.9	1	1	-0.99
8V	0.69	0.80	1.23	0.45	1.9	1	1	-1.08
8M	0.84	0.90	1.25	0.36	1.8	1	1	-0.85
95	0.61	0.96	1.06	0.57	1.6	1	1	-0.62
3	0.75	1.05	1.00	0.00	1.2	1	1	-0.18
2	0.63	0.66	1.14	0.46	1.8	1	1	-1.10
1	0.50	1.25	1.14	0.46	2.0	1	1	-0.71
91	0.70	2.41	1.50	0.42	25	-	1,2	-
AVG	0.74	1.39	1.25	0.41	1.87	-	-	-

Violation of Geometric Assumptions from Parametric Study			
ID#	n Predicted	n Actual	Geometric Assumptions Met?
47	1	2	no: Multi-Lobular, Elongated Neck, CrsSctn Ellipticity
21	1	2	no: Side Bleb
61	2	2	no: Multi-Lobular, High Curvature in Centerline
51	2	2	no: Multi-Lobular, Plane Angle
7	2	2	no: Plane Angle, Top Bleb
54	2	2	no: CrsSctn Ellipticity
15	2	2	no: CrsSctn Ellipticity
6	2	2	no: Plane Angle
98	1	1	no: Top Bleb
66	1	1	no: Top Bleb
32	1	1	no: CrsSctn Ellipticity
68	1	1	no: Top Bleb
4	1	1	no: CrsSctn Ellipticity
5	2	2	yes
87	2	2	yes
78	1	1	yes
49	1	1	yes
96	1	1	yes
20	1	1	yes
11	1	1	yes
8V	1	1	yes
8	1	1	yes
95	1	1	yes
3	1	1	yes
2	1	1	yes
1	1	1	yes
91	-	1,2	no: Two Domes

BIBLIOGRAPHY

[1.] Laaksamo, E., Tulamo, R., Liiman, A., Baumann, M., Friedlander, R., Hernesniemi, J., Kangasniemi, M. Niemelä, M., Laakso, A., Frösen, J., 2012, "Oxidative Stress Is Associated With Cell Death,Wall Degradation, and Increased Risk of Rupture of the Intracranial Aneurysm Wall," Neurosurgery 72:109–117

[2.] Nader-Sepahi, A., Casimiro, M., Sen, J., and Kitchen, N. D., 2004, "Is aspect ratio a reliable predictor of intracranial aneurysm rupture?," Neurosurgery, 54(6), pp. 1343-1347

[3.] Weir, B., Amidei, C., Kongable, G., Findlay, J. M., Kassell, N. F., Kelly, J., Dai, L., and Karrison, T. G., 2003, "The aspect ratio (dome/neck) of ruptured and unruptured aneurysms.," Journal of Neurosurgery, 99(3), pp. 447-451.

[4.] Malek, A. M., Alper, S. L., and Izumo, S., 1999, "Hemodynamic shear stress and its role in atherosclerosis," JAMA, 282(21), pp. 2035-2042.

[5.] Shojima, M., Oshima, M., Takagi, K., Torii, R., Hayakawa, M., Katada, K., Morita, A., and Kirino, T., 2004, "Magnitude and role of wall shear stress on cerebral aneurysm: computational fluid dynamic study of 20 middle cerebral artery aneurysms," Stroke, 35(11), pp. 2500-2505.

[6.] Kaiser, D., Freyberg, M., and Friedl, P., 1997, "Lack of Hemodynamic Forces Triggers Apoptosis in Vascular Endothelial Cells," Biochemical and Biophysical Research Communications 231, 586-590 Article No. RC976246

[7.] Pentimalli L, Modesti A, Vignati A, et al., 2004 "Role of apoptosis in intracranial aneurysm rupture. J Neurosurg.";101(6):1018-1025.

[8.] Cebral, J. R., Castro, M. A., Burgess, J. E., Pergolizzi, R. S., Sheridan, M. J., and Putman, C. M., 2005, "Characterization of Cerebral Aneurysms for Assessing Risk of Rupture By Using Patient-Specific Computational Hemodynamics Models," AJNR Am J Neuroradiol, 26(10), pp. 2550-2559.

[9.] Ujiie, H., Tachibana, H., Hiramatsu, O., Hazel, A. L., Matsumoto, T., Ogasawara, Y., Nakajima, H., Hori, T., Takakura, K., and Kajiya, F., 1999, "Effects of size and shape (aspect ratio) on the hemodynamics of saccular aneurysms: a possible index for surgical treatment of intracranial aneurysms," Neurosurgery, 45(1), pp. 119-129; discussion 129-130.

[10.] Ujiie, H., Tachibana, H., Hiramatsu, O., Hazel, A. L., Matsumoto, T., Ogasawara, Y., Nakajima, H., Hori, T., Takakura, K., and Kajiya, F., 1999, "Effects of size and shape (aspect ratio) on the

hemodynamics of saccular aneurysms: a possible index for surgical treatment of intracranial aneurysms," Neurosurgery, 45(1), pp. 119-129; discussion 129-130.

[11.] Beck J, Rohde S, el Beltagy M et al (2003) Difference in configuration of ruptured and unruptured intracranial aneurysms determined by biplanar digital subtraction angiography. Acta Neurochir (Wien) 145:861–865.

[12.] Raghavan, M. L., Ma, B., and Harbaugh, R. E., 2005, "Quantified aneurysm shape and rupture risk," Journal of Neurosurgery, 102(2), pp. 355-362.

[13.] Zeng, Z., Durka, M.J., Kallmes, D. F., Ding, Y., and Robertson, A. M., 2011, "Can aspect ratio be used to categorize intra-aneurysmal hemodynamics?- A study of elastase induced aneurysms in rabbit," Journal of Biomechanics 44 (2011) 2809–2816.

[14.] Zakaria, H., Robertson, A. M., and Kerber, C. W., 2008, "A parametric model for studies of flow in arterial bifurcations," Ann Biomed Eng, 36(9), pp. 1515-1530.

[15.] Zeng, Z., 2011, "Novel methodologies for investigating the pathophysiology of cerebral aneurysms", Doctoral Dissertation, University of Pittsburgh

[16.] Zeng, Z., Kallmes, D. F., Durka, M. J., Ding, Y., Lewis, D., Kadirvel, R., and Robertson, A. M., 2011, "Hemodynamics and anatomy of elastase-induced rabbit aneurysm models-similarity with human cerebral aneurysms?," AJNR Am J Neuroradiol, March, 32: 595 - 601.

[17.] Frösen, J., Tulamo, R., Paetau, A., Laaksamo, E., Korja, M., Laakso, A., Niemelä, M., Hernesniemi, J., 2012, "Saccular intracranial aneurysm: pathology and mechanisms" Acta Neuropathol (2012) 123:773–786.

[18.] Parlea, L., Fahrig, R., Holdsworth, D. W., and Lownie, S. P., 1999, "An analysis of the geometry of saccular intracranial aneurysms," Ajnr: American Journal of Neuroradiology, 20(6), pp. 1079-1089.